Cell Chemical Biology

# Noncanonical *Streptococcus sanguinis* ComCDE circuitry integrates environmental cues in transformation outcome decision

## Graphical abstract

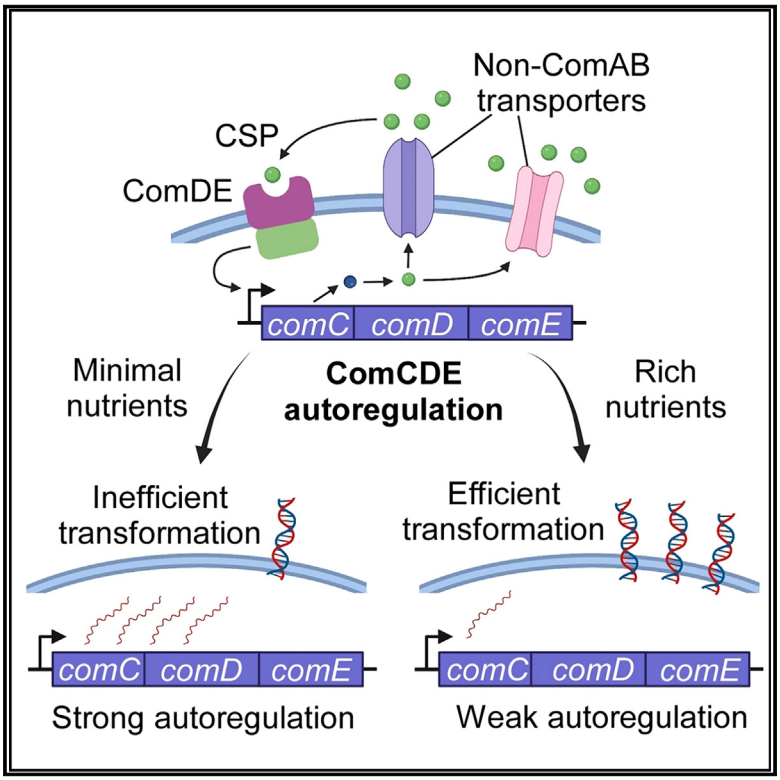


## Authors

Mingzhe Guo, Clay P. Renshaw, Ryan W. Mull, Yftah Tal-Gan

## Correspondence

ytalgan@unr.edu

## In brief

Guo et al. discovered the two CSP exporters in *Streptococcus sanguinis* through a combination of genome-wide mutagenesis and synthetic approaches. The intensity of *S. sanguinis* ComCDE autoregulation can be impacted by environmental inputs, where it is inversely related to the outcome of competence-mediated transformation.

## Highlights

- *S. sanguinis* utilizes two host ABC transporters for CSP export
- Disrupting *S. sanguinis* ComCDE autoregulation results in hyperefficient competence
- *S. sanguinis* produces a bacteriocin that primarily targets gram-positive bacteria

Guo et al., 2024, Cell Chemical Biology *31*, 1–14
February 15, 2024 
https://doi.org/10.1016/j.chembiol.2023.09.007

CellPress

Cell Chemical Biology

CellPress

Article

# Noncanonical *Streptococcus sanguinis* ComCDE circuitry integrates environmental cues in transformation outcome decision

Mingzhe Guo,[1] Clay P. Renshaw,[1] Ryan W. Mull,[1] and Yftah Tal-Gan[1,2,*]
[1]Department of Chemistry, University of Nevada, Reno, 1664 N. Virginia St, Reno, NV 89557, USA
[2]Lead contact
*Correspondence: ytalgan@unr.edu
https://doi.org/10.1016/j.chembiol.2023.09.007

## SUMMARY

Natural competence is the principal driver of streptococcal evolution. While acquisition of new traits could facilitate rapid fitness improvement for bacteria, entry into the competent state is a highly orchestrated event, involving an interplay between various pathways. We present a new type of competence-predation coordination mechanism in *Streptococcus sanguinis*. Unlike other streptococci that mediate competence through the ComABCDE regulon, several key components are missing in the *S. sanguinis* ComCDE circuitry. We assembled two synthetic biology devices linking competence-stimulating peptide (CSP) cleavage and export with a quantifiable readout to unravel the unique features of the *S. sanguinis* circuitry. Our results revealed the ComC precursor cleavage pattern and the two host ABC transporters implicated in the export of the *S. sanguinis* CSP. Moreover, we discovered a ComCDE-dependent bacteriocin locus. Overall, this study presents a mechanism for commensal streptococci to maximize transformation outcome in a fluid environment through extensive circuitry rewiring.

## INTRODUCTION

The composition of the oral microbiome harbors immense ramifications for human health. Oral microbiome dysbiosis can not only trigger pathogenesis in the immediate vicinity, including dental caries and periodontitis, but can also contribute to systemic diseases via ectopic vegetation (e.g., bacteremia) or still cryptic mechanisms such as diabetes, cancer, and Alzheimer's disease.[1–3] Streptococci shape the assembly of the oral microbiome as pioneer colonizers that influence the adhesion of subsequent occupants.[4] *Streptococcus sanguinis* epitomizes the duality of oral streptococci comprising the commensal flora. On the one hand, it is one of the most abundant streptococci species that colonizes the surface of the tooth, with copious clinical evidence associating the presence of *S. sanguinis* with increased oral health.[5,6] This feature is primarily attributed to its ability to antagonize *S. mutans* and other periodontal pathogens.[7,8] On the other hand, despite its overall benign disposition, *S. sanguinis* is also capable of mounting systemic infection when seeded into the bloodstream through dental surgery or minor lesions formed from daily routines.[9] Due to its peculiar affinity to platelet,[10] *S. sanguinis* can colonize the heart valve and is therefore a leading cause of endocarditis.[11]

Natural genetic transformation is the lynchpin for horizontal gene transfer among streptococci, which is the main driving factor behind their genome plasticity. Acquisition of foreign genetic materials accelerates evolution, including the retention and spread of antibiotic resistance genes. Competence development in streptococci is mediated by the alternative sigma factor ComX (SigX).[12] Sustaining the competent state exacts a high fitness cost for the bacteria because nutrients and cellular machineries are diverted from essential activities.[13] To mitigate the deleterious repercussion and maximize transformation efficiency, entry into competence and its concomitant shutoff are tightly regulated.[14,15] There are two exclusive pheromone-based cell-density communication (quorum sensing) systems overseeing ComX regulation.[16] For members in the mutans, pyogenic, and bovis groups of streptococci, ComX is subject to the control of the ComRS system.[1,17–23] In the mitis, anginosus, and sanguinis groups of streptococci, induction of SigX is under the regulation of the ComCDE circuitry. The CSP (competence-stimulating peptide) precursor, ComC, is cleaved and exported by an ABC transporter complex, ComAB. On the extracellular membrane, upon reaching a threshold concentration, the diffused CSP can bind and activate its cognate histidine kinase receptor, ComD. Consequently, ComD undergoes autophosphorylation, resulting in subsequent phosphorylation and activation of the response regulator ComE. Phosphorylated ComE then activates *comX* transcription as well as *comCDE* autoregulation. *S. sanguinis* possesses a rewired ComCDE system (Figure S1A). First, the identity of the *S. sanguinis* CSP has been elusive due to its ComC lacking the Gly-Gly cleavage motif that is ubiquitous in other ComC sequences.[24] Second, how the *S. sanguinis* ComC is cleaved and transported remains a mystery due to its lack of an apparent ComAB exporter.[25]

Please cite this article in press as: Guo et al., Noncanonical *Streptococcus sanguinis* ComCDE circuitry integrates environmental cues in transformation outcome decision, Cell Chemical Biology (2023), https://doi.org/10.1016/j.chembiol.2023.09.007



Due to the polymicrobial nature of the oral microbiome, streptococci utilize multiple offensive measures to carve out their particular niche in this defined environment. A majority of oral streptococci produce hydrogen peroxide.[4,26] Streptococci also employ a highly heterogeneous repertoire of antimicrobial bacteriocins.[27] In most model streptococci species, bacteriocin biogenesis is mediated by the *blp* gene cluster, which is often linked with the competence regulon. Some notable exceptions have been discovered in *S. salivarius*, where bacteriocin regulation is extensively rewired.[28,29] While bioinformatics approaches have not identified any bacteriocin genes in the *S. sanguinis* genome, there is evidence suggesting that there is active bacteriocin production.[30,31]

In this study, we elucidated these unique traits of *S. sanguinis* by introducing several novel approaches. First, we validated the *S. sanguinis* CSP by harnessing the autoregulatory nature of the ComCDE regulon. Second, we exploited a ComC overexpression-induced growth defect to study its cleavage pattern. Third, through a proxy measurement of CSP export, we discovered that *S. sanguinis* CSP is preferentially exported by two ABC transporters. Notably, we found that competence efficiency spiked when *comCDE* autoregulation was impaired. We also unearthed a ComE-activated bacteriocin biosynthesis cluster that produces a substance with broad-spectrum antimicrobial activity. Lastly, we discovered that an autocrine-like ComCDE signaling propagation resulting from inefficient cell-to-cell communication can drastically improve the transformation efficiency. Our results fill long standing gaps in our understanding of the particulars of the ComCDE circuitry in *S. sanguinis* and demonstrate a new strategy for commensal streptococci to capture external DNA more efficiently in a complex environment.

## RESULTS

### Confirmation of native *S. sanguinis* CSP

The identity of the *S. sanguinis* CSP has never been confirmed, although a 15mer peptide derived from the *S. sanguinis* ComC sequence was found to activate the ComCDE regulon.[32] To narrow down the potential CSP candidates, we first tested the competence-activating ability of several synthetic CSP candidates derived from the *S. sanguinis* ComC sequence, starting from the *C*-terminal end of the sequence and varying the peptide length (13–21 amino acid residues) by including additional residues at the *N*-terminal region. To this end, we constructed a new *S. sanguinis* reporter strain containing the firefly luciferase *luc* gene under the control of the *comCDE* promoter and used it to test the activity of the different CSP candidates. Our results revealed that only the 15mer and 16mer sequences could activate the *comCDE* locus (Figure 1A).

Next, we sought to confirm the native CSP sequence by extracting it from overnight *S. sanguinis* culture.[33,34] Unfortunately, peptide masses corresponding to 15mer or 16mer CSP could not be detected in the spent media. The difficulty in isolating the *S. sanguinis* native CSP is likely the result of either a) *S. sanguinis* CSP production is intrinsically low or b) *S. sanguinis* CSP is sequestered rapidly.[35] To circumvent these potential issues, we proposed to isolate the native CSP through artificial induction (Figure 1B). Our setup was based on the autoregulatory nature of the ComCDE circuitry and the fact that there should only be a single native CSP sequence. Since the *S. sanguinis* ComC-derived 15mer and 16mer CSP derivatives were similarly active, they should both be able to induce the production of the native sequence. Our results revealed that only the 15mer peptide could be retrieved from the diluted culture treated with the 15mer peptide, whereas both the 15mer and 16mer peptides were retrieved from the diluted culture treated with the 16mer, suggesting that the 15mer peptide should be the *bona fide S. sanguinis* native CSP sequence (Figure 1C). To exclude the possibility of the involvement of a membrane-bound protease in the 15mer formation following 16mer treatment, we first tried to induce the diluted *S. sanguinis* culture with the inactive 17mer and 18mer peptides. However, in both cases, we did not detect the mass of the 15mer peptide (Figure 1C). Furthermore, we synthesized a 15mer CSP that contains a deuterium-labeled leucine (L-Leucine D10) and used it to induce native CSP production. Following peptide extraction, the MS results revealed the presence of a non-deuterated 15mer CSP in the supernatant (Figure S1G). Therefore, we concluded that the putative 15mer we obtained following either 16mer or deuterated 15mer treatment is the direct result of the *comCDE* autoregulation.

We then proceeded to validate the identity of the native CSP by comparing the analytical high-performance liquid chromatography (HPLC) profiles of synthetic 15mer and extracted CSP. Both samples displayed identical retention time, as did the 1:1 mixture of the two samples (Figure 1D). Lastly, we performed mass spectrometry analysis of both the native and synthetic 15mer CSP peptides to verify the sequence identity of the extracted peptide. The obtained spectra for both peptides yielded 100% sequence identity between the two peptides (Figure 1E and Table S2). In conclusion, we devised a robust protocol to isolate native streptococci CSPs and confirmed the identity of the native *S. sanguinis* CSP.

### *S. sanguinis* ComC cleavage is mediated by the Thr-Phe-Trp motif

Mignolet et al. recently demonstrated that activation of the ComRS pathway in *S. salivarius* induces a growth defect phenotype.[29] We reasoned that if *S. sanguinis* ComE activation exerts a similar effect, we can harness this phenotype to probe the cleavage mechanism of *S. sanguinis* ComC by linking artificial growth defect with mutagenesis screening of ComC. Surprisingly, we found that *S. sanguinis* ComC overexpression can induce a significant growth defect while direct CSP treatment cannot (Figure 2A).

While SigX-inducing peptide (XIP) treatment could elicit growth defect in *S. salivarius*, addition of CSP could not produce a similar effect in *S. sanguinis*. To resolve this inconsistency, we tried to pinpoint the source of ComC overexpression-induced growth defect. To this end, we removed either the 19 AAs prior to the CSP (del 2–20) or the terminal arginine (del 35) in the ComC overexpression construct. In the ComC del 2–20 mutant, the CSP is expected to be released to the supernatant without the need of cleavage, whereas in the ComC del 35 mutant, the cleavage is still expected to occur to produce a significantly less-potent 14mer CSP analog lacking the *C*-terminal AA (Figure S1). First, to evaluate whether the different ComC overexpression constructs produce active CSP, we quantified the presence of functional CSP in the supernatant from strains harboring

Please cite this article in press as: Guo et al., Noncanonical *Streptococcus sanguinis* ComCDE circuitry integrates environmental cues in transformation outcome decision, Cell Chemical Biology (2023), https://doi.org/10.1016/j.chembiol.2023.09.007





A

| Compound | Sequence | $EC_{50}$(nM) | 95%CI |
|---|---|---|---|
| 13mer | RGVPNPWGWIFGR | N.A | N.A |
| 14mer | LRGVPNPWGWIFGR | N.A | N.A |
| 14mer(Des-R15) | DLRGVPNPWGWIFG | 79.9 | 29.7-130 |
| 15mer | DLRGVPNPWGWIFGR | 14.4 | 4.87-23.9 |
| 16mer | WDLRGVPNPWGWIFGR | 4.09 | 2.84-5.33 |
| 17mer | FWDLRGVPNPWGWIFGR | N.A | N.A |
| 18mer | TFWDLRGVPNPWGWIFGR | N.A | N.A |
| 19mer | QTFWDLRGVPNPWGWIFGR | N.A | N.A |
| 20mer | VQTFWDLRGVPNPWGWIFGR | N.A | N.A |
| 21mer | LVQTFWDLRGVPNPWGWIFGR | N.A | N.A |

B

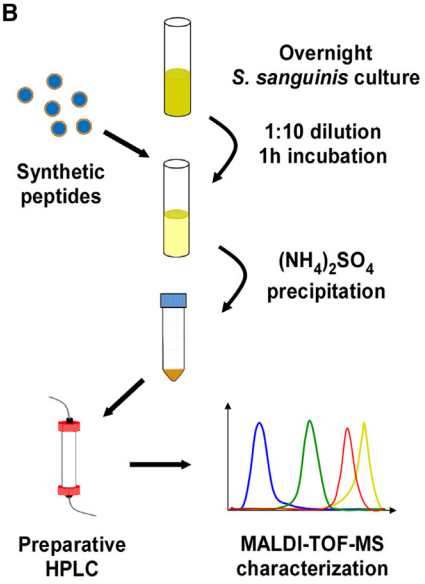


C

| Input synthetic peptides | Recovered peptides | | | |
|---|---|---|---|---|
| | 15mer | 16mer | 17mer | 18mer |
| 15mer | + | - | - | - |
| 16mer | + | + | - | - |
| 17mer | - | - | + | - |
| 18mer | - | - | - | + |

D

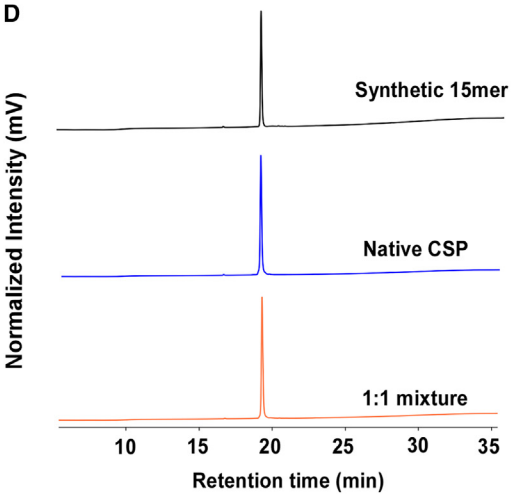


E

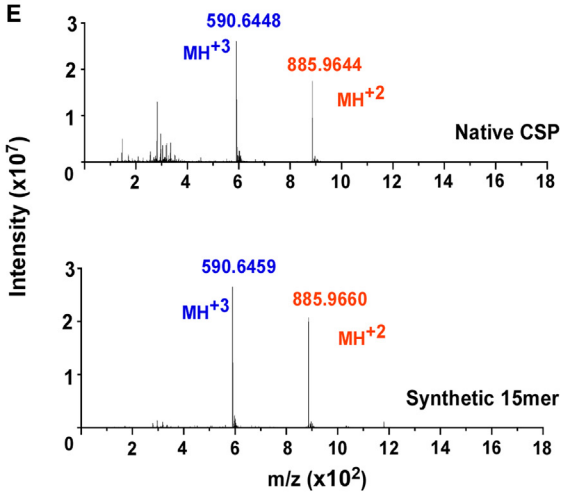


**Figure 1. Confirmation of natural *S. sanguinis* CSP**

(A) The *comCDE*-activating capability of a series of *S. sanguinis* CSP candidates was determined through the *S. sanguinis* indicator strain containing $P_{comCDE}$luc construct (see Figure S1 for details).

(B) Illustration of native *S. sanguinis* CSP isolation workflow.

(C) Comparison of recovered peptide profiles from diluted *S. sanguinis* culture treated with various synthetic peptides.

(D) Comparison of analytical HPLC profiles of native *S. sanguinis* CSP, synthetic *S. sanguinis* 15mer, and 1:1 mixture of the two.

(E) Exact mass spectra of isolated and synthetic CSP exhibiting masses that correspond to both a +2 and a +3 charge states of the native *S. sanguinis* CSP.

different ComC constructs using a newly constructed Δ*comC*-$p_{comCDE}$-*luc* reporter system. Our results revealed that functional CSP can be detected in both the wild-type (WT) ComC and ComC del 2–20 constructs, but not in the ComC del 35 construct (Figures S2A and S2B).

Next, we proceeded to test the growth defect-inducing capability of these new ComC mutant constructs. Our results revealed that the ComC del 35 construct induces a significant growth defect, while the ComC del 2–20 construct does not (Figure S2C). These results suggest that the growth defect originates from processing of ComC itself, not the downstream signaling cascade. To further validate this hypothesis, we tested the growth defect-inducing capability of WT-ComC overexpression construct in both Δ*comCDE* and Δ*comX* backgrounds. Our results indicate that overexpression of WT ComC induces a strong growth defect without competence activation (Figure S2C). We also transformed the WT-ComC and ComC del 2–20 constructs into the integrative $p_{comCDE}$-*luc* reporter background and recorded the $OD_{600}$ and luminescence continuously. The results revealed that competence activation can only occur after *S. sanguinis* exit the lag phase (Figures S2D and S2E), despite the constant presence of active CSP in the supernatant. The ComC overexpression-induced growth defect manifests as a long lag phase, further validating that the growth defect is not

Please cite this article in press as: Guo et al., Noncanonical *Streptococcus sanguinis* ComCDE circuitry integrates environmental cues in transformation outcome decision, Cell Chemical Biology (2023), https://doi.org/10.1016/j.chembiol.2023.09.007



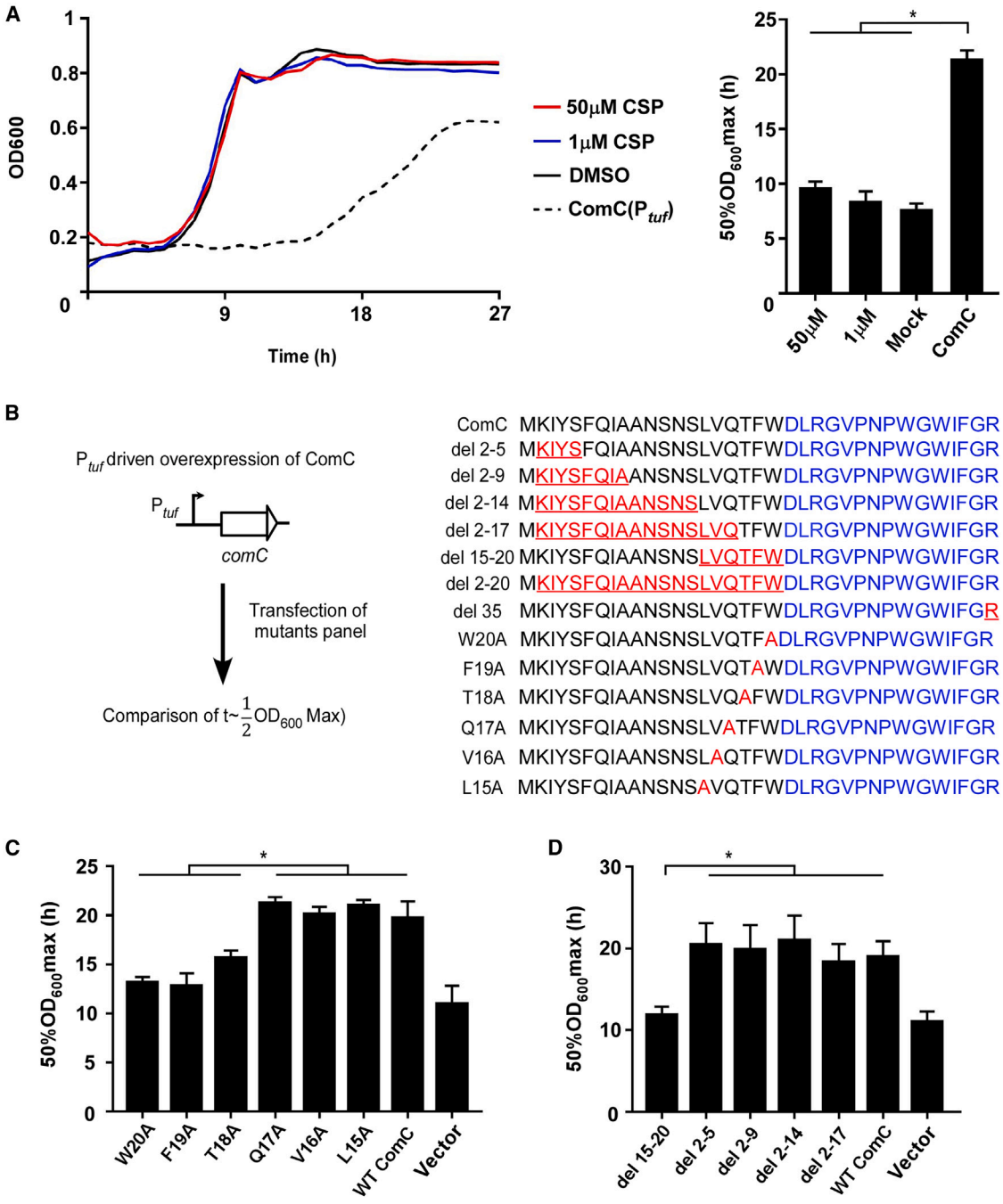


**Figure 2. *S. sanguinis* ComC cleavage pattern**

(A) Left panel, growth curves of diluted *S. sanguinis* cultures treated with CSP of various concentrations or *S. sanguinis* strain containing a *comC* overexpression construct driven by the promoter of the housekeeping gene *tuf*. Right panel, comparison of the time required for *S. sanguinis* cultures in the left panel to reach 50% of maximal $OD_{600}$. Each curve is a mean of three independent replicates. *$p < 0.05$.

(B) Left panel, schematic of the workflow linking *S. sanguinis* ComC overexpression with growth defect. WT ComC and its mutant series were overexpressed in *S. sanguinis* constitutively. Then, 50% of maximal $OD_{600}$ was used as the readout to indicate a growth defect. Right panel, illustration of the AAs sequences of the panel of ComC mutants.

(C and D) Comparison of the time required for each *S. sanguinis* strain harboring respective ComC mutant to reach 50% of maximal $OD_{600}$. The values are represented as the mean of three independent replicates with standard deviation, *$p < 0.05$.

Please cite this article in press as: Guo et al., Noncanonical *Streptococcus sanguinis* ComCDE circuitry integrates environmental cues in transformation outcome decision, Cell Chemical Biology (2023), https://doi.org/10.1016/j.chembiol.2023.09.007





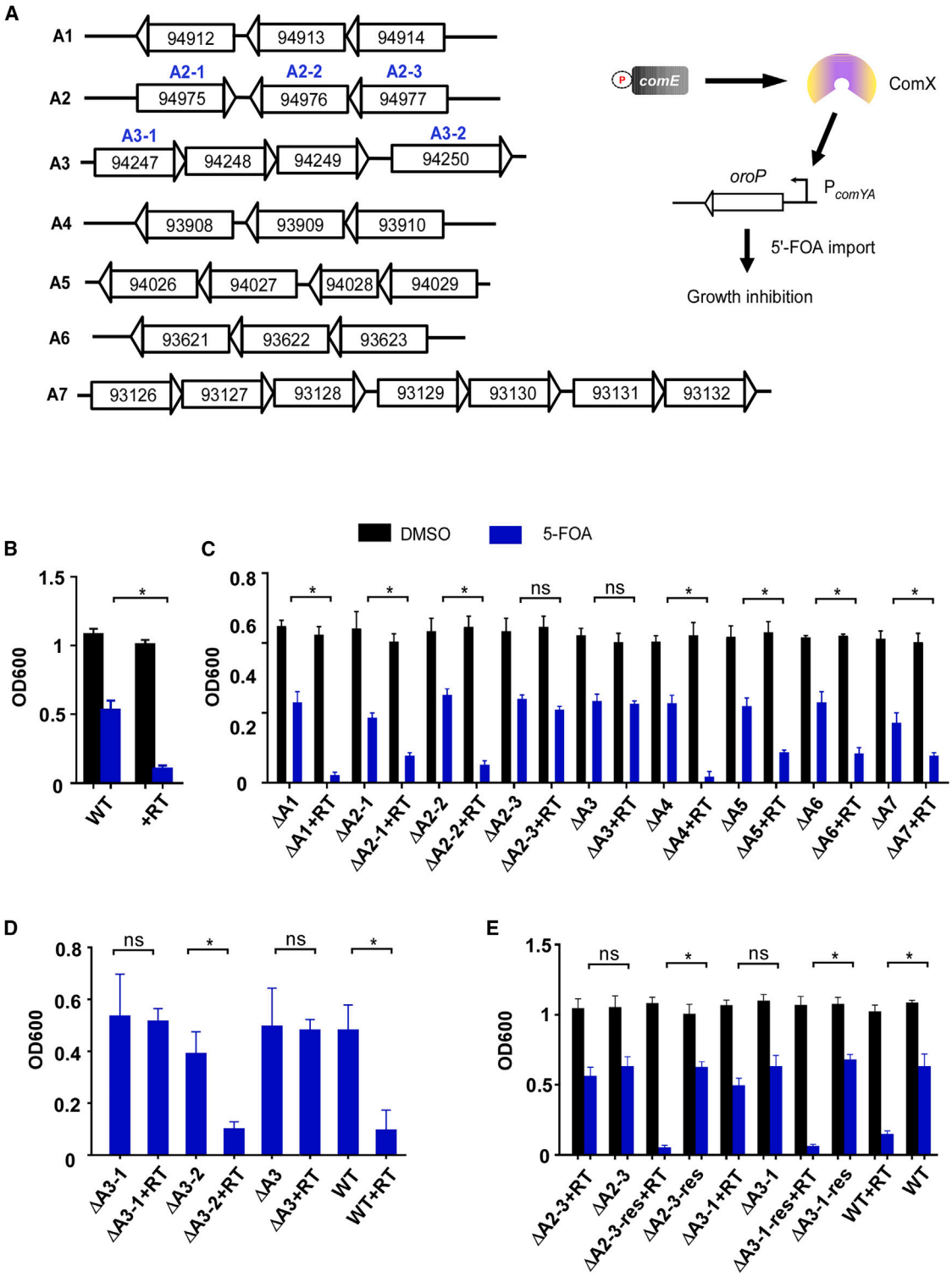


**Figure 3. *S. sanguinis* CSP is secreted by two ABC transporters**

(A) Left panel, schematics of multiple *S. sanguinis* ABC transporter clusters that were selected for knockout. Right panel, creation of the toxicity reporter linking competence activation with growth defect where the OroP transporter was subject to the control of the promoter of a late *S. sanguinis* competence gene *comYA*.

(B) Comparison of $OD_{600}$ of *S. sanguinis* with (+RT) or without toxicity reporter 12 h after DMSO or 5′-FOA treatment. *$p < 0.05$.

*(legend continued on next page)*

Please cite this article in press as: Guo et al., Noncanonical *Streptococcus sanguinis* ComCDE circuitry integrates environmental cues in transformation outcome decision, Cell Chemical Biology (2023), https://doi.org/10.1016/j.chembiol.2023.09.007



related to competence. In conclusion, we have identified the cleavage of the ComC precursor as the main driver of this artificial ComC overexpression-related growth defect.

Since the growth defect observed in *S. sanguinis* originates from *comC* on the plasmid construct, we deduced that abrogation of the ComC cleavage site by mutating the *comC* gene on the plasmid construct can reverse this growth defect. Therefore, we created a panel of $P_{tuf}$ *comC* mutant constructs (Figure 2B) and transformed *S. sanguinis* with them. Next, we compared the growth defect of these *S. sanguinis* strains. Of the six amino acid residues adjacent to the CSP sequence, alanine substitution at positions 18, 19, or 20 abolished the growth defect, while alanine substitution at positions 15, 16, or 17 retained the growth defect phenotype observed using a plasmid bearing WT ComC (Figure 2C). These results suggest that the three amino acid residues directly preceding the CSP sequence constitute the recognition motif for ComC cleavage.

To further probe the role of the ComC *N*-terminal region in CSP processing, we tested the growth profile of another series of *S. sanguinis* $P_{tuf}$ *comC* mutant strains with various *N*-terminal deletions. The results indicate that *S. sanguinis* ComC can be cleaved even after extensive *N*-terminal deletion (del 2–17); however, the removal of the last six amino acid residues directly preceding the CSP sequence (del 15–20) abolished CSP processing (Figure 2D). Together, these results point out to the Thr-Phe-Trp motif directly adjacent to the CSP sequence as the recognition motif for ComC cleavage and CSP maturation.

## *S. sanguinis* CSP is secreted by two ABC transporters

The lack of ComAB counterparts in *S. sanguinis* suggests that the mature CSP is transported by non-dedicated ABC transporters. A major challenge in identifying the unknown transporter is the lack of a convenient readout that could be adapted in a large-scale knockout screening. To address this issue, we devised a proxy measurement of CSP export by coupling activation of the *comCDE* locus with artificial toxicity generation. By attaching the promoter of a late competence gene *comYA* in front of *oroP*, competence activation could drive the expression of the OroP transporter, which selectively imports 5′-fluoroorotic acid (FOA), resulting in DNA synthesis inhibition (Figure 3A). Our results indicated that the toxicity reporter driven by natural competence could induce significant growth defect in WT *S. sanguinis* background (Figures 3B and S3).

To screen for the CSP transporter, we combined the toxicity reporter with an extensive ABC transporter knockout (Δ) screening. First, we downloaded all the annotated *S. sanguinis* ABC transporter entries from the UniProt database. After manual mapping and curating, the *S. sanguinis* ABC transporters were partitioned into seven clusters (Figure 3A). For convenience, we initially tried to create seven respective *S. sanguinis* ABC transporter cluster (A1-A7) deletion strains. We obtained six *S. sanguinis* cluster deletion strains—all except for the A2 cluster. Interestingly, A2-1, A2-2, and A2-3 individual deletion could be obtained. Next, we transformed the obtained ABC transporter deletion panel with the toxicity reporter and probed their growth in the presence of 5′-FOA. The results revealed competence-coupled growth defects in most transporter deletion strains, except for the ΔA2-3 and A3 cluster deletion strains (Figures 3C and S3). We next proceeded to create individual deletion strains within the A3 cluster and transformed the ΔA3-1 and ΔA3-2 strains with the toxicity reporter. The results indicated that the competence-coupled growth defect is abolished in ΔA3-1 but not ΔA3-2 (Figure 3D). Complementation of the respective transporters back into the ΔA3-1 and ΔA2-3 strains restored their sensitivity to 5′-FOA toxicity (Figure 3E). In conclusion, we successfully utilized our competence-toxicity coupling approach to identify the two ABC transporters involved in *S. sanguinis* CSP export.

## Attenuation of *comCDE* autoregulation boosts competence

Since CSP is transported by the two ABC transporters (A3-1, A2-3), we hypothesized that loss of either one of the two transporters would lead to reduced CSP export and global attenuation of competence gene activation. First, we measured the CSP-releasing capability of various *S. sanguinis* transporter deletion backgrounds using the Δ*comC*-$p_{comCDE}$-*luc* reporter system. Our results indicate that deletion of either the A2-3 or the A3-1 transporter leads to less efficient CSP export, as the CSP concentration in these backgrounds was significantly lower than that of the WT (Figure S4A). Next, we determined the expression kinetics of *comE* mRNA in different transporter deletion backgrounds by qRT-PCR. In the WT strain, full *comCDE* activation could be sustained by autoregulation for at least 50 min. Moreover, in a Δ*comC* background, following initial activation caused by the addition of exogenous CSP, autoregulation was abolished immediately after (Figure S4B). As expected, in the ΔA3-1 and ΔA2-3 backgrounds, CSP export impairment rendered the autoregulation less effective, where *comE* mRNA levels were significantly below that of the WT after 30 min (Figure 4A). It is worth pointing out that in the ΔA3-1 and ΔA2-3 dual deletion background, the *comCDE* autoregulation is severely inhibited, where the *comE* peak expression shifted to around 20 min post CSP treatment and the maximal peak expression was attenuated (Figure 4A). Since knocking out the entire A2 cluster yielded a non-viable strain, it could possibly be that the double knockout strain lacking both A3-1 and A2-3 suffers from stress induced by impaired core cellular functions.

Expression kinetics of *comX* were different from those of *comE*. The *comX* expression peaked at 10 min post CSP treatment and remained relatively stable over the next 40 min (Figure 4B). In the Δ*comC* background, *comX* mRNA level was reduced to background level by 30 min after CSP treatment (Figure S4B). Surprisingly, similar alternation in expression kinetics in the single transporter deletion strains was not observed for *comX* mRNA. Contrarily, the double transporter deletion strain

(C) Comparison of $OD_{600}$ of a panel of *S. sanguinis* ABC transporter cluster knockout strains with or without toxicity reporter 12 h after DMSO or 5′-FOA treatment. *$p < 0.05$.
(D) Comparison of $OD_{600}$ of a panel of *S. sanguinis* ABC transporter knockout strains with or without toxicity reporter 12 h after 5′-FOA treatment. *$p < 0.05$.
(E) Comparison of $OD_{600}$ of two of *S. sanguinis* ABC transporter knockout strains harboring toxicity reporter with or without its complement ABC transporter rescue 12 h after DMSO or 5′-FOA treatment. The values are represented as the mean of three independent replicates with standard deviation. *$p < 0.05$.

Please cite this article in press as: Guo et al., Noncanonical *Streptococcus sanguinis* ComCDE circuitry integrates environmental cues in transformation outcome decision, Cell Chemical Biology (2023), https://doi.org/10.1016/j.chembiol.2023.09.007





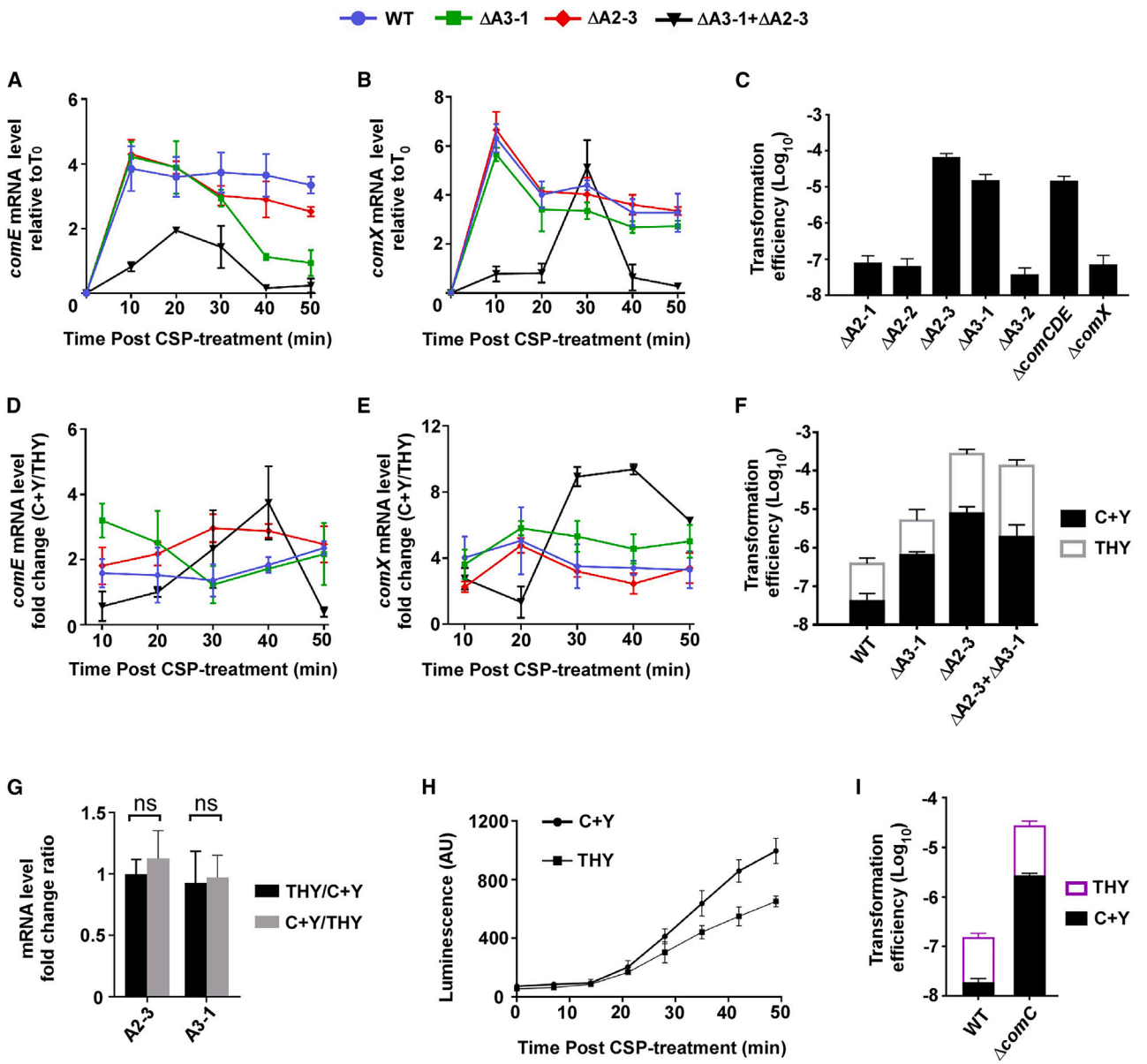


**Figure 4. Attenuation of *comCDE* autoregulation boosts competence**

(A) Comparison of *comE* mRNA level in various ABC transporter deletion *S. sanguinis* strains by qRT-PCR. Values are presented as the ratio of expression level between various time points and time point zero in units of $\log_2$. All values are represented as the mean of three independent replicates with standard deviation.

(B) Comparison of *comX* mRNA level in various ABC transporter deletion strains by qRT-PCR. Values are presented as the ratio of expression level between various time points and time point zero in units of $\log_2$. All values are represented as the mean of three independent replicates with standard deviation.

(C) Comparison of transformation efficiency of *S. sanguinis* transformed with 10 ng of various linear knockout cassettes. All values are represented as the mean of three independent replicates with standard deviation.

(D) Comparison of *comE* mRNA level in various ABC transporter deletion *S. sanguinis* strains by qRT-PCR. Values are presented as the ratio of expression level between that in C + Y and in THY (C + Y/THY) at each time point in units of $\log_2$. All values are represented as the mean of three independent replicates with standard deviation.

(E) Comparison of *comX* mRNA level in various ABC transporter deletion strains by qRT-PCR. Values are presented as the ratio of expression level between that in C + Y and in THY (C + Y/THY) at each time point in units of $\log_2$. All values are represented as the mean of three independent replicates with standard deviation.

(F) Comparison of transformation efficiency of various ABC transporter deletion *S. sanguinis* strains in different nutritional states (THY vs. C + Y). All values are represented as the mean of three independent replicates with standard deviation.

(G) Comparison of A2-3/A3-1 mRNA levels using qRT-PCR in WT *S. sanguinis* when shifting between the two nutritional states (THY to C + Y, and vice versa). Values are presented as the ratio of expression level between that in the specific media (i.e., C + Y) and the shifted media (i.e., C + Y to THY). All values are represented as the mean of three independent replicates with standard deviation.

*(legend continued on next page)*

Please cite this article in press as: Guo et al., Noncanonical *Streptococcus sanguinis* ComCDE circuitry integrates environmental cues in transformation outcome decision, Cell Chemical Biology (2023), https://doi.org/10.1016/j.chembiol.2023.09.007



again exhibited a delay in *comX* peak expression to around 30 min, similar to the delay in *comE* expression, followed by an immediate drop in intensity. We noticed that exogenous CSP-induced transformation of WT *S. sanguinis* with either linear deletion cassette (A2-3 or A3-1) yielded an unusually high number of antibiotic-resistant colonies compared to transforming the deletion cassettes corresponding to the other transporters, resulting in significantly higher transformation efficiency (Figure 4C). We reasoned that this counterintuitive observation may be the result of one of two scenarios: either the competence shutoff mechanism is mediated by some early or late competence genes, or the attenuation of *comCDE* autoregulation directly leads to increased transformation efficiency. If the first option is true, the attenuation of the primary competence circuitry switch through impaired CSP export would dampen the competence shutoff and prolong the transformation window, leading to a higher transformation efficiency. We believe this scenario is unlikely based on our qRT-PCR results. Since *comX* expression levels are comparable between the WT and the single transporter deletion backgrounds, the expression profile of late competence genes should be uniform as well. As for other early competence genes, based on previous microarray data,[32] there are only six early competence genes in *S. sanguinis* SK36: *comCDE*, *comX*, *SSA_1889*, and *SSA_0195*, and the latter two genes are not involved in competence development. Therefore, the only observed phenotype derived from CSP transporter deletion is the attenuation of *comCDE* autoregulation, and we propose that this phenomenon is directly responsible for the spike in competence efficiency.

We therefore hypothesized that all manners of *comCDE* autoregulation disruption would lead to similar increases in competence efficiency. Indeed, the *S. sanguinis* CSP transporter deletions inflict global *comCDE* autoregulation impairment, and both the ΔA2-3 and ΔA3-1 strains, as well as the ΔA3-1 and ΔA2-3 dual deletion strain, display a hyperefficiency phenotype when undergoing CSP-induced DNA transformation (Figure 4F). Interestingly, the transformation efficiency in the ΔA3-1 and ΔA2-3 dual deletion background is on par with that of ΔA2-3, suggesting that this ABC transporter is the dominant CSP transporter. To further validate our hypothesis, we sought to create a localized *comCDE* autoregulation defect by transforming *S. sanguinis* with a deletion cassette corresponding to the *comCDE* locus. As expected, upon exogenous CSP-induced transformation of WT *S. sanguinis* with linear *comCDE* deletion cassette, but not upon transformation with linear *comX* deletion cassette, an unusually high number of transformants were observed, resulting in higher transformation efficiency (Figure 4C). While we do not fully understand why impairment of ComCDE autoregulation would cause that spike in transformation efficiency, there is the possibility that the genomic loci of the putative CSP exporters or of *comCDE* are uniquely positioned to the effect that interaction with external DNA is more favored.

Previous studies in *S. mutans* and *S. pneumoniae* indicated that media composition could affect competence induction through differential regulation of transport and degradation of autoinducers.[20,36,37] Notably, the membrane-bound protease, HtrA, could degrade *S. mutans and S. pneumoniae* CSP; however, this process is inhibited by small peptides present in complex medium. Since most *S. sanguinis* strains possess HtrA homologs (data not shown), we speculated that the media composition could also impact CSP metabolism. To test this hypothesis, we compared the expression kinetics of *S. sanguinis comE* and *comX* under CSP induction in C + Y media. Surprisingly, the qPCR results indicated that *comCDE* autoregulation was consistently stronger in C + Y media than in THY media across all time points and genetic backgrounds (Figure 4D), as were the kinetics of *comX* mRNA (Figure 4E). Consistent with our previous results where autoregulation inhibition boosted transformation efficiency, elevated *comCDE* autoregulation under C + Y media was associated with a drop in transformation efficiency, suggesting that the nutrition landscape itself could modulate the transformation outcome in *S. sanguinis* (Figure 4F).

To further elucidate the mechanism by which the media composition affects transformation, we first determined the ratio of A2-3 and A3-1 mRNA levels when shifting between the two different media, THY to C + Y, and vice versa. The results indicated that the expression level of these two transporters remains stable during media shift (Figure 4G). Next, we tested whether the stronger mRNA induction observed in C + Y media is associated with stronger CSP production or transcriptional activity. Therefore, we utilized the Δ*comC*$p_{ComCDE}$-luc *S. sanguinis* strain, where endogenous CSP production is eliminated, to evaluate ComCDE activation following exogenous CSP treatment through luminescence. The results revealed that CSP-induced luminescence is consistently higher in C + Y than in THY media (Figure 4H). Coupled with the mRNA levels shown in Figures 4D and 4E, one or more components in the C + Y media render the ComCDE autoregulation more efficient at the transcriptional level. Consistent with the previously observed pattern where ComCDE autoregulation is reversely correlated to transformation outcome, the transformation efficiency was found to be much higher in the Δ*comC* background than in WT for both nutritional states (Figure 4I).

Overall, our results suggest that disruption of cell-to-cell communication mediated by the ComCDE signaling pathway, either by disrupting ComC production/export or via a shift in the nutritional microenvironment, can impact transformation efficiency.

## *S. sanguinis* ComE activates a bacteriocin biosynthesis cluster

To determine whether *S. sanguinis* produces any bacteriocin, we first created a Δ*spxB S. sanguinis* strain, in which hydrogen peroxide production is abolished. We then performed a classic spot-on-lawn assay, where saturated *S. sanguinis* culture was spotted on a lawn formed by *Lactococcus lactis*. The assay exhibited a growth inhibition ring where *S. sanguinis* culture was spotted, suggesting the presence of a bacteriocin (Figure 5A).

(H) Comparison of luminescence in different media conditions (C + Y and THY) following exogenous CSP treatment. The synthetic CSP was added into Δ*comC S. sanguinis* strain containing the $p_{ComCDE}$-luc reporter in two media conditions (C + Y and THY), and luminescence was recorded every 10 min post CSP treatment for a total of 50 min. All values are represented as the mean of three independent replicates with standard deviation.

(I) Comparison of transformation efficiency of WT *S. sanguinis* and Δ*comC S. sanguinis* strains transformed with 10 ng of pDL278 blank plasmid in different nutritional states (THY vs. C + Y). All values are represented as the mean of three independent replicates with standard deviation.

Please cite this article in press as: Guo et al., Noncanonical *Streptococcus sanguinis* ComCDE circuitry integrates environmental cues in transformation outcome decision, Cell Chemical Biology (2023), https://doi.org/10.1016/j.chembiol.2023.09.007





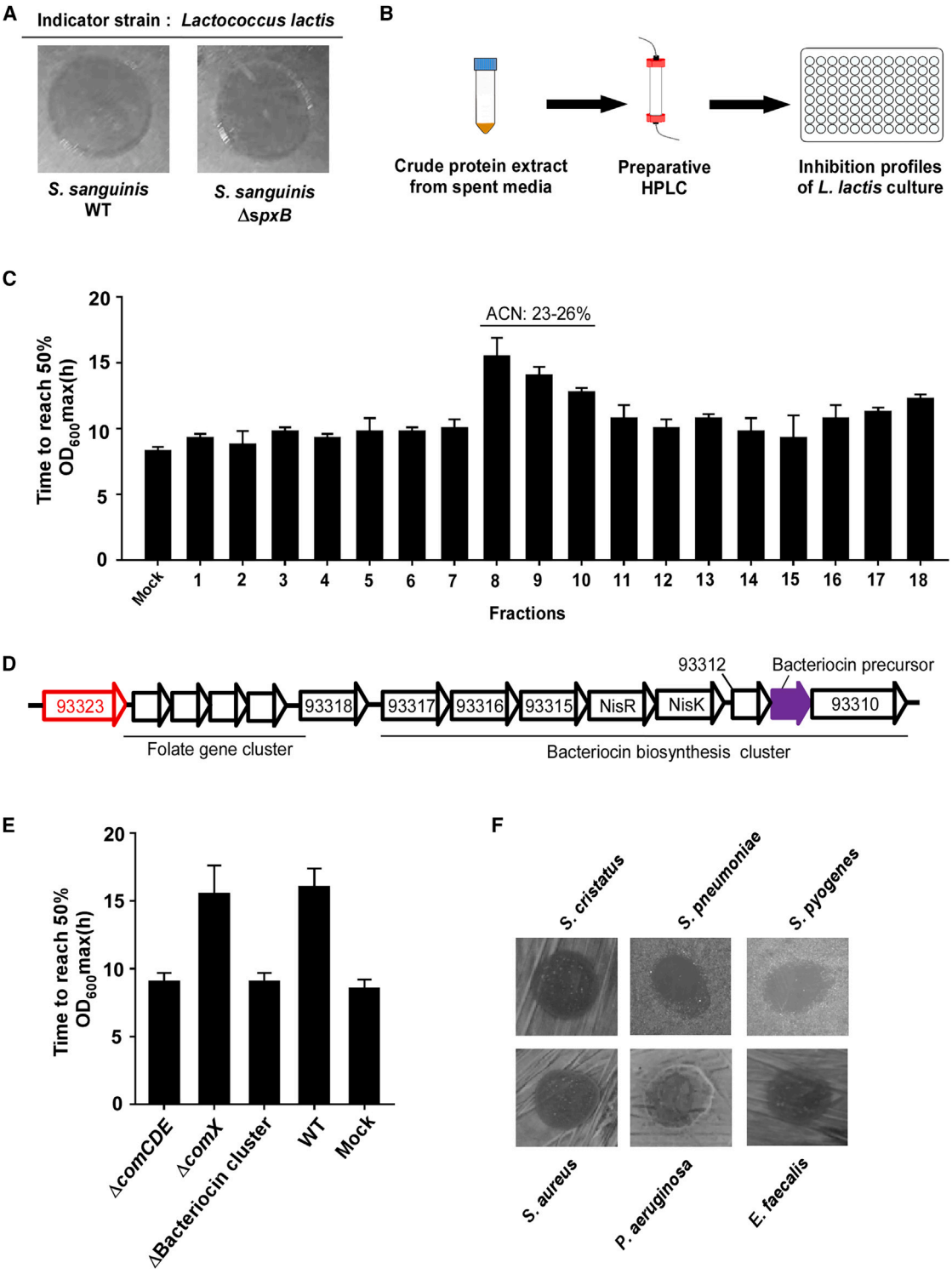


**Figure 5. *S. sanguinis* ComE activates a bacteriocin biosynthesis cluster**

(A) Lawns were created with indicator strain *L. lactis* on a THY plate, 10 μL of *S. sanguinis* or *S. sanguinis* Δ*spxB* overnight cultures were spotted onto the top of the indicator lawn.

(B) Schematics of HPLC-based characterization of antimicrobial properties of crude peptide contents from spent *S. sanguinis* media.

(C) Fractions collected from preparative HPLC separation of crude peptide extracted from overnight *S. sanguinis* culture were lyophilized and dissolved with 100 μL THY media, 50 μL of which were mixed with 150 μL diluted *L. lactis* culture. Then, growth kinetics were recorded with an automated plate reader. The time

*(legend continued on next page)*

Please cite this article in press as: Guo et al., Noncanonical *Streptococcus sanguinis* ComCDE circuitry integrates environmental cues in transformation outcome decision, Cell Chemical Biology (2023), https://doi.org/10.1016/j.chembiol.2023.09.007



Next, we tried to pinpoint the identity of the *S. sanguinis* bacteriocin combining HPLC and phenotypic assay (Figure 5B). We noticed that fractions eluted between 23% and 26% acetonitrile (ACN) significantly inhibited *L. lactis* growth (Figures 5C and S5).

Since the predation behavior in streptococci is generally dependent on the primary competence circuitry, we speculated that *S. sanguinis* bacteriocin production is subject to ComCDE regulation as well. To verify this hypothesis, we utilized the Δ*comCDE* and Δ*comX S. sanguinis* strains we created and determined the respective inhibition capacity of the peptide content eluted between 23% and 26% ACN for each of the supernatants. The results indicated that bacteriocin production was attenuated in the Δ*comCDE* background, while the Δ*comX* does not affect the inhibition capability (Figure 5E). Thus, the bacteriocin locus is under the direct control of ComE and should have the expression profile of an early competence gene.

We therefore examined the early competence genes of *S. sanguinis* VMC66, the strain we use, and found that downstream of one of the early competence genes, 93323, there is a folate biosynthesis cluster and a cluster that resembles a nisin lantibiotic cluster (Figure 5D). To test whether this nisin-like cluster is responsible for bacteriocin production, and consequently the observed *L. lactis* inhibition, we created a deletion strain of the cluster (Δbacteriocin cluster) and found that *L. lactis* inhibition was abolished (Figure 5E). Thus, *S. sanguinis* produces a bacteriocin through a novel biosynthesis cluster relying on ComE activation. To further validate the regulatory link between the ComCDE circuitry and the bacteriocin cluster, we examined the organization of the whole biosynthesis cluster and found it to be divided into two sub-clusters with two distinctive promoter regions: sub-cluster 1 from 93317-NisK and sub-cluster 2 from 93311-bacteriocin precursor-93310. We hypothesized that if the bacteriocin cluster could be activated by competence induction, one of the two bacteriocin sub-clusters should display mRNA expression profile resembling that of the early competence regulon, while the other sub-cluster should display a delayed mRNA activation kinetics. To validate this hypothesis, we measured the mRNA expression kinetics of two genes, one from each sub-cluster. The results reveal that the expression kinetics of *nisR* peaks at 10 min post CSP treatment, indicating that CSP induces the activation of the biosynthesis sub-cluster 1 (Figure S6D). As for biosynthesis sub-cluster 2, the expression kinetics of the bacteriocin precursor peaks at around 20–30 min post CSP treatment, indicating that activation of sub-cluster 2 lags that of sub-cluster 1. The mRNA expression profiles of *nisR* and bacteriocin precursor in the Δ*comX* background are similar to those of WT *S. sanguinis*, while a complete loss of activation of the two bacteriocin sub-clusters is observed in the Δ*comCDE* background (Figure S6D). Together, these results point to the involvement of the ComCDE circuitry at the very start.

We speculated that the early colonizer status of *S. sanguinis* may be attributed to the antimicrobial activity of the *S. sanguinis* bacteriocin. To test this hypothesis, we spotted redissolved peptide contents derived from the HPLC fractions collected between 23% and 26% ACN on various THY agar plates with pre-streaked lawns formed by a variety of bacterial pathogens. Our results indicate that the *S. sanguinis* bacteriocin can inhibit a variety of streptococci, including two clinically relevant species, *S. pneumoniae* and *S. pyogenes* (Figures 5F and S6B). We need to point out that *S. sanguinis* bacteriocin failed to produce a recognizable inhibition halo on the *S. mutans* lawn (Figure S6A). Yet, the *S. sanguinis* bacteriocin was able to slow down the growth rate of *S. mutans* culture (Figure S5D), suggesting that *S. mutans* may have evolved defense mechanisms against this antimicrobial agent.

Next, we tested the susceptibilities of a variety of other gram-positive and gram-negative bacterial species to the *S. sanguinis* bacteriocin. Interestingly, several gram-positive bacterial species were found to be susceptible to the *S. sanguinis* bacteriocin, including the notorious pathogens *Staphylococcus aureus* and vancomycin-resistant *Enterococcus faecalis* (Figure 5F). We noticed that the *S. sanguinis* bacteriocin was also able to inhibit the growth rate of diluted methicillin resistance *S. aureus* culture while not producing an inhibition halo in the spot-on-lawn assay (Figures S5E and S6A). Of all the gram-negative bacteria we tested, the *S. sanguinis* bacteriocin could only generate an inhibition ring on a *Pseudomonas aeruginosa* lawn (Figures 5F and S6A), suggesting that this antimicrobial agent is mainly effective against gram-positive species. Overall, we demonstrated that *S. sanguinis* competence activation induces the biosynthesis of a bacteriocin whose wide-spectrum antimicrobial activity may confer *S. sanguinis* with a decisive advantage during the establishment of the oral flora.

## DISCUSSION

Previous studies indicated that CSP maturation does not necessarily occur following the double-glycine motif in the ComC precursor, as cleavage can take place out of its immediate vicinity or secondary cleavage can follow in tandem.[33,38–40] Thus, it is important to determine the actual identity of streptococci CSP experimentally. Unfortunately, for various streptococci species, we found it to be very difficult to isolate the CSP directly from the overnight culture (data not shown). We speculated that is due to the fitness cost tethered to competent state maintenance, which ensures that the competence circuitry is only briefly maintained during a specific growth stage in most circumstances. This type of stringent control on competence regulon stipulates that CSP is also produced and secreted transiently, which may explain the observed difficulty in isolating the native CSP.

required for each well to reach 50% of maximal $OD_{600}$ was selected as the readout to assess the inhibition capability of each fraction. All values are represented as the mean of three independent replicates with standard deviation.

(D) Illustration of the configuration of the bacteriocin biosynthesis cluster.

(E) Contents eluted between 23% and 26% ACN from preparative HPLC separation of crude peptide extracts derived from overnight culture of various *S. sanguinis* backgrounds were lyophilized and dissolved in 100 μL THY media, 50 μL of which were mixed with 150 μL diluted *L. lactis* culture, and growth kinetics were recorded with an automated plate reader. The time required for each well to reach 50% of maximal $OD_{600}$ was selected as the readout to assess the inhibition capability of the fraction. All values are represented as the mean of three independent replicates with standard deviation.

(F) Lawns were created with respective indicator strains on a THY plate. 10 μL of putative *S. sanguinis* bacteriocin purified from spent *S. sanguinis* media was spotted onto the top of the respective indicator lawns. The image was taken after overnight incubation.

Please cite this article in press as: Guo et al., Noncanonical *Streptococcus sanguinis* ComCDE circuitry integrates environmental cues in transformation outcome decision, Cell Chemical Biology (2023), https://doi.org/10.1016/j.chembiol.2023.09.007





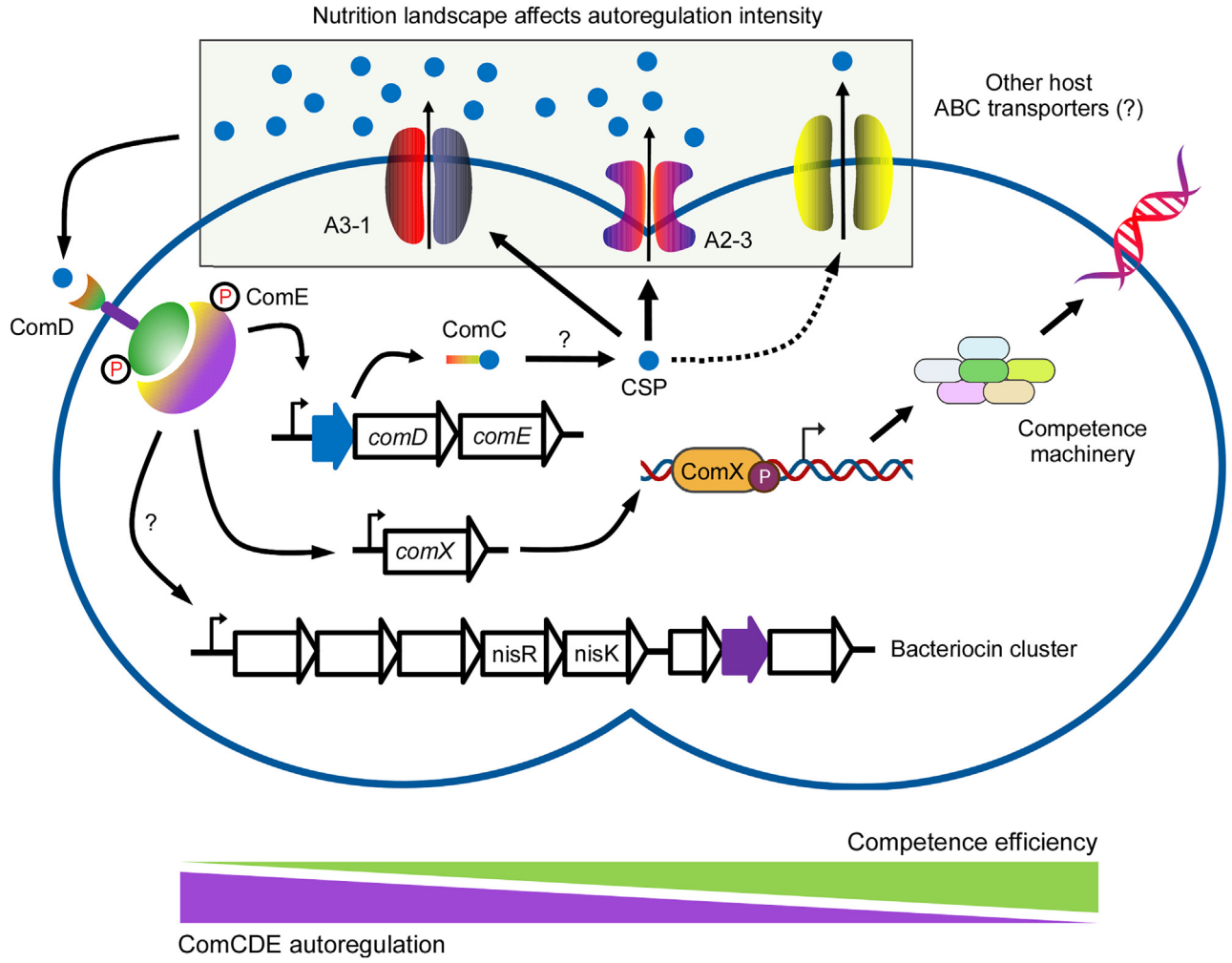


**Figure 6. Rewiring of *S. sanguinis* competence circuitry confers flexible control of transformation outcome**

The competence system in *S. sanguinis* possesses some notable differences from other streptococcal species. First, the *S. sanguinis* ComC precursor is cleaved by a still unknown host peptidase and the mature CSP is preferably exported by the two host ABC transporters, A2-3 and A3-1. Second, our work demonstrates that when ComCDE autoregulation is disrupted, the transformation efficiency uniformly increased. The most physiological relevant example of this feature is that the nutritional composition of the media can impact ComCDE autoregulation, suggesting that oral streptococcal species can modulate DNA intake through a shift in the nutritional landscape. Lastly, the *S. sanguinis* competence cascade can trigger the activation of a bacteriocin biosynthesis cluster.

Instead of trying to capture this narrow window that permits activation of the competence circuitry, we utilized the autoregulatory nature of the ComCDE circuitry. As long as the input synthetic peptide, which is different from the actual CSP, retains competence-activating capacity, the resultant native CSP can be easily separated from the input synthetic peptide by HPLC and its identity confirmed via mass spectrometry. Since most ComRS systems are also subject to autoregulation, we believe this approach can be readily adapted for XIP identification as well.

It has been well documented that overactivation of the competence circuitry can induce growth defects.[29] There are at least three known approaches to recapitulate this phenotype: 1) overexpression of a primary competence switch, 2) synthetic pheromone treatment, or 3) overexpression of pheromone/precursor. Surprisingly, in our case, synthetic CSP treatment, even at high concentration, could not affect *S. sanguinis* growth, whereas ComC overexpression drastically altered the growth curve of *S. sanguinis* diluted culture. We can now explain this discrepancy with the discoveries in our study that ComC processing can prolong the lag phase, while competence activation can only be initiated after the exit of lag phase. It is worth pointing out that CSP is constantly in surplus in these ComC overexpression backgrounds, while extra time is required for *S. sanguinis* CSP to accumulate in its native condition. Therefore, it will be interesting to see if this link between growth stage and competence activation stays the same in the natural environment. While we do not know the molecular mechanism behind this regulatory link, it might be the deleterious consequences associated with excessive ComC expression that necessitate this type of stringent control. The most peculiar aspect about *S. sanguinis* ComC overexpression-induced growth defect is that it originates upstream of ComCDE signaling, possibly due to cleavage of the ComC precursor. The most likely scenario is that the host peptidase involved in ComC maturation is also processing substrates

Please cite this article in press as: Guo et al., Noncanonical *Streptococcus sanguinis* ComCDE circuitry integrates environmental cues in transformation outcome decision, Cell Chemical Biology (2023), https://doi.org/10.1016/j.chembiol.2023.09.007



that are vital for survival of the host. Therefore, overexpression of ComC saturates the peptidase, resulting in disruption of cellular growth. Another possibility is that the free *N*-terminal region of the *S. sanguinis* ComC that precedes the CSP has a biological function of its own, and its accumulation results in a growth defect. Either way, this unique feature of *S. sanguinis* ComC suggests that widespread rewiring of the competence circuitry to different extents exists in streptococci.

Wang et al. have previously shown that in *S. pneumoniae*, CSP export can overlap with bacteriocin export, resulting in CSP being exported by both ComAB/BlpAB.[41] The most important consequence of CSP export by BlpAB is the enhancement of competence induction. This enhancement in competence induction indicates that CSP transporter expression level is a rate-limiting factor for CSP secretion and competence activation in streptococci utilizing a canonical ComABCDE configuration. *S. sanguinis* utilizes two host ABC transporters for CSP export, whose expression levels are not associated with competence induction (Figure 6). It is worth noting that based on InterPro prediction, the two identified *S. sanguinis* CSP exporters likely do not possess peptidase activity. Thus, cleavage of the ComC precursor is possibly carried out by an unknown host peptidase, resembling that of ComS. Overall, the function of ComAB is carried out by host machinery in *S. sanguinis*. Therefore, the *S. sanguinis* ComCDE circuitry has one less rate-limiting factor compared to its canonical Com ABCDE counterparts. Instead, the ComCDE circuitry in *S. sanguinis* resembles that of the ComRS system, where cleavage and export is decoupled from the competence circuitry. This ComCDE rewiring possibly confers faster initiation kinetics of *S. sanguinis* competence activation, as well as expedite the deployment of the *S. sanguinis* bacteriocin, allowing *S. sanguinis* to act as an effective early colonizer.

The chemical nature of the *S. sanguinis* bacteriocin is still undetermined; however, it is almost certain to be different from nisin bacteriocins for several reasons. First, the putative *S. sanguinis* bacteriocin precursor shares no homology with any of the existing known nisin analogs (Figure S6C). Second, the configuration of the *S. sanguinis* bacteriocin biosynthetic cluster, which lacks a protease and a modifying enzyme, is highly different from a canonical nisin lantibiotic cluster. This evidence suggests that the mature *S. sanguinis* bacteriocin is 54 AA long and contains no posttranslational modifications. It is worth pointing out that the 93315, 93316, and 93317 genes in the *S. sanguinis* bacteriocin biosynthesis cluster are predicted to be putative bacteriocin permeases through protein BLAST. Coupled with the result that bacteriocin activity can be observed in the double deletion of putative CSP exporters background (Figure S6E), we can infer that CSP transport and bacteriocin export are two independent processes. While the *S. sanguinis* bacteriocin could be developed into a novel drug against multidrug-resistant gram-positive bacteria, clinical *S. sanguinis* isolates likely cannot be utilized directly as a probiotic due to *S. sanguinis* association with endocarditis. To overcome this issue, the *S. sanguinis* bacteriocin biosynthetic pathway can be engineered into other, relatively non-pathogenic commensal species as a means to combat dysbiosis-induced pathogenesis.

### Limitations of the study

First, our results indicated that *S. sanguinis* CSP could be exported in the background of dual deletion of the two CSP transporters, suggesting that *S. sanguinis* CSP could be exported passively in certain conditions. Second, although the bacteriocin promoters do not contain the canonical ComE-binding motif, MEME prediction indicates that there are several motifs shared by promoters of early competence genes and the bacteriocin cluster. As a result, we do not know whether ComE activates bacteriocin biosynthesis directly or indirectly. Third, we rely on ComC overexpression to study the regulatory link between growth stage and competence activation. Therefore, we should exercise caution when applying our finding to the natural condition where CSP accumulation is much slower. Lastly, we tried to identify the host protease responsible for ComC cleavage via transposon screening in the $P_{tuf}$ *comC* background. However, we failed to find a suppressor mutant in which ComC-induced growth defect is abolished. We hypothesize that this is because the unknown protease is essential, and thus, its deletion cannot be tolerated. Future screening of this host factor may have to rely on gain of function.

## SIGNIFICANCE

**_S. sanguinis_, a ubiquitous commensal, promotes a dental-caries-free environment by shaping the oral microbiome composition as a pioneer colonizer. _S. sanguinis_ can integrate extracellular DNA by entering into a competent state mediated through an evolutionarily divergent ComCDE competence regulon system. Our work unravels the key components of this unique pathway and uncovers a competence-concerted predation behavior. Specifically, in response to global impairment of _comCDE_ autoregulation, stemming from a shift in nutrient landscape or population heterogeneity, _S. sanguinis_ exhibits enhanced transformation efficiency. This mechanism likely confers _S. sanguinis_ with higher evolutionary plasticity over its neighbors in the oral cavity. Overall, this study reports a model where streptococci could benefit from alteration in competence signaling in response to environmental cues.**

## STAR★METHODS

Detailed methods are provided in the online version of this paper and include the following:

- KEY RESOURCES TABLE
- RESOURCE AVAILABILITY
  - Lead contact
  - Materials availability
  - Data and code availability
- EXPERIMENTAL MODEL AND STUDY PARTICIPANT DETAILS
  - Bacterial growth
  - Strain construction
- METHOD DETAILS
  - Solid-phase peptide synthesis, HPLC, and mass spectrometry
  - Isolation of native *S. sanguinis* CSP
  - Luminescence assays
  - Plasmid construction
  - RNA isolation and quantification
  - Competition assays on solid medium

## SUPPLEMENTAL INFORMATION

Supplemental information can be found online at https://doi.org/10.1016/j.chembiol.2023.09.007.

## ACKNOWLEDGMENTS

This work was supported by a grant from the National Institutes of Health (R35GM128651). Research reported in this publication made use of the University of Nevada, Reno (UNR) Cellular and Molecular Imaging (CMI) core facility supported by the National Institute of General Medical Sciences of the National Institutes of Health under grant number P30 103650.

## AUTHOR CONTRIBUTIONS

M.G. constructed strains and performed experiments; M.G. and Y.T. designed experiments and analyzed data; M.G. and Y.T. wrote the original draft; C.P.R., R.W.M., and Y.T. reviewed and edited subsequent manuscript versions. C.P.R. contributed by MS/MS experiments. Y.T. supervised all aspects of the project.

## DECLARATION OF INTERESTS

The authors declare no competing financial interest.

Received: January 19, 2023
Revised: July 25, 2023
Accepted: September 18, 2023
Published: October 12, 2023

## REFERENCES

1. Amer, A., Galvin, S., Healy, C.M., and Moran, G.P. (2017). The Microbiome of Potentially Malignant Oral Leukoplakia Exhibits Enrichment for Fusobacterium, Leptotrichia, Campylobacter, and Rothia Species. Front. Microbiol. *8*, 2391. https://doi.org/10.3389/fmicb.2017.02391.
2. Schmidt, B.L., Kuczynski, J., Bhattacharya, A., Huey, B., Corby, P.M., Queiroz, E.L.S., Nightingale, K., Kerr, A.R., DeLacure, M.D., Veeramachaneni, R., et al. (2014). Changes in abundance of oral microbiota associated with oral cancer. PLoS One *9*, e98741. https://doi.org/10.1371/journal.pone.0098741.
3. Pushalkar, S., Ji, X., Li, Y., Estilo, C., Yegnanarayana, R., Singh, B., Li, X., and Saxena, D. (2012). Comparison of oral microbiota in tumor and non-tumor tissues of patients with oral squamous cell carcinoma. BMC Microbiol. *12*, 144. https://doi.org/10.1186/1471-2180-12-144.
4. Baty, J.J., Stoner, S.N., and Scoffield, J.A. (2022). Oral Commensal Streptococci: Gatekeepers of the Oral Cavity. J. Bacteriol. *204*, e0025722. https://doi.org/10.1128/jb.00257-22.
5. Kreth, J., Giacaman, R.A., Raghavan, R., and Merritt, J. (2017). The road less traveled - defining molecular commensalism with Streptococcus sanguinis. Mol. Oral Microbiol. *32*, 181–196. https://doi.org/10.1111/omi.12170.
6. Treerat, P., Redanz, U., Redanz, S., Giacaman, R.A., Merritt, J., and Kreth, J. (2020). Synergism between Corynebacterium and Streptococcus sanguinis reveals new interactions between oral commensals. ISME J. *14*, 1154–1169. https://doi.org/10.1038/s41396-020-0598-2.
7. Giacaman, R.A., Torres, S., Gómez, Y., Muñoz-Sandoval, C., and Kreth, J. (2015). Correlation of Streptococcus mutans and Streptococcus sanguinis colonization and ex vivo hydrogen peroxide production in carious lesion-free and high caries adults. Arch. Oral Biol. *60*, 154–159. https://doi.org/10.1016/j.archoralbio.2014.09.007.
8. Herrero, E.R., Slomka, V., Bernaerts, K., Boon, N., Hernandez-Sanabria, E., Passoni, B.B., Quirynen, M., and Teughels, W. (2016). Antimicrobial effects of commensal oral species are regulated by environmental factors. J. Dent. *47*, 23–33. https://doi.org/10.1016/j.jdent.2016.02.007.
9. Nobbs, A., and Kreth, J. (2019). Genetics of sanguinis-Group Streptococci in Health and Disease. Microbiol. Spectr. *7*. https://doi.org/10.1128/microbiolspec.GPP3-0052-2018.
10. Martini, A.M., Moricz, B.S., Woods, L.J., and Jones, B.D. (2021). Type IV Pili of Streptococcus sanguinis Contribute to Pathogenesis in Experimental Infective Endocarditis. Microbiol. Spectr. *9*, e0175221. https://doi.org/10.1128/Spectrum.01752-21.
11. Callahan, J.E., Munro, C.L., and Kitten, T. (2011). The Streptococcus sanguinis competence regulon is not required for infective endocarditis virulence in a rabbit model. PLoS One *6*, e26403. https://doi.org/10.1371/journal.pone.0026403.
12. Luo, P., Li, H., and Morrison, D.A. (2003). ComX is a unique link between multiple quorum sensing outputs and competence in Streptococcus pneumoniae. Mol. Microbiol. *50*, 623–633. https://doi.org/10.1046/j.1365-2958.2003.03714.x.
13. Zaccaria, E., Wells, J.M., and van Baarlen, P. (2016). Metabolic Context of the Competence-Induced Checkpoint for Cell Replication in Streptococcus suis. PLoS One *11*, e0153571. https://doi.org/10.1371/journal.pone.0153571.
14. Veening, J.W., and Blokesch, M. (2017). Interbacterial predation as a strategy for DNA acquisition in naturally competent bacteria. Nat. Rev. Microbiol. *15*, 621–629. https://doi.org/10.1038/nrmicro.2017.66.
15. Claverys, J.P., and Håvarstein, L.S. (2007). Cannibalism and fratricide: mechanisms and raisons d'etre. Nat. Rev. Microbiol. *5*, 219–229. https://doi.org/10.1038/nrmicro1613.
16. Fontaine, L., Wahl, A., Fléchard, M., Mignolet, J., and Hols, P. (2015). Regulation of competence for natural transformation in streptococci. Infect. Genet. Evol. *33*, 343–360. https://doi.org/10.1016/j.meegid.2014.09.010.
17. Khan, R., Rukke, H.V., Ricomini Filho, A.P., Fimland, G., Arntzen, M.Ø., Thiede, B., and Petersen, F.C. (2012). Extracellular identification of a processed type II ComR/ComS pheromone of Streptococcus mutans. J. Bacteriol. *194*, 3781–3788. https://doi.org/10.1128/JB.00624-12.
18. Desai, K., Mashburn-Warren, L., Federle, M.J., and Morrison, D.A. (2012). Development of competence for genetic transformation of Streptococcus mutans in a chemically defined medium. J. Bacteriol. *194*, 3774–3780. https://doi.org/10.1128/JB.00337-12.
19. Talagas, A., Fontaine, L., Ledesma-García, L., Mignolet, J., Li de la Sierra-Gallay, I., Lazar, N., Aumont-Nicaise, M., Federle, M.J., Prehna, G., Hols, P., and Nessler, S. (2016). Structural Insights into Streptococcal Competence Regulation by the Cell-to-Cell Communication System ComRS. PLoS Pathog. *12*, e1005980. https://doi.org/10.1371/journal.ppat.1005980.
20. Reck, M., Tomasch, J., and Wagner-Döbler, I. (2015). The Alternative Sigma Factor SigX Controls Bacteriocin Synthesis and Competence, the Two Quorum Sensing Regulated Traits in Streptococcus mutans. PLoS Genet. *11*, e1005353. https://doi.org/10.1371/journal.pgen.1005353.
21. Gardan, R., Besset, C., Gitton, C., Guillot, A., Fontaine, L., Hols, P., and Monnet, V. (2013). Extracellular life cycle of ComS, the competence-stimulating peptide of Streptococcus thermophilus. J. Bacteriol. *195*, 1845–1855. https://doi.org/10.1128/JB.02196-12.
22. Lingeswaran, A., Metton, C., Henry, C., Monnet, V., Juillard, V., and Gardan, R. (2020). Export of Rgg Quorum Sensing Peptides is Mediated by the PptAB ABC Transporter in Streptococcus Thermophilus Strain LMD-9. Genes *11*, 1096. https://doi.org/10.3390/genes11091096.
23. Kaspar, J., Underhill, S.A.M., Shields, R.C., Reyes, A., Rosenzweig, S., Hagen, S.J., and Burne, R.A. (2017). Intercellular Communication via the comX-Inducing Peptide (XIP) of Streptococcus mutans. J. Bacteriol. *199*, e00404–e00417. https://doi.org/10.1128/JB.00404-17.
24. Håvarstein, L.S., Hakenbeck, R., and Gaustad, P. (1997). Natural competence in the genus Streptococcus: evidence that streptococci can change

pherotype by interspecies recombinational exchanges. J. Bacteriol. *179*, 6589–6594. https://doi.org/10.1128/jb.179.21.6589-6594.1997.

25. Xu, P., Alves, J.M., Kitten, T., Brown, A., Chen, Z., Ozaki, L.S., Manque, P., Ge, X., Serrano, M.G., Puiu, D., et al. (2007). Genome of the opportunistic pathogen Streptococcus sanguinis. J. Bacteriol. *189*, 3166–3175. https://doi.org/10.1128/JB.01808-06.
26. Kreth, J., Merritt, J., Shi, W., and Qi, F. (2005). Competition and coexistence between Streptococcus mutans and Streptococcus sanguinis in the dental biofilm. J. Bacteriol. *187*, 7193–7203. https://doi.org/10.1128/JB.187.21.7193-7203.2005.
27. Vogel, V., and Spellerberg, B. (2021). Bacteriocin Production by Beta-Hemolytic Streptococci. Pathogens *10*, 867. https://doi.org/10.3390/pathogens10070867.
28. Mignolet, J., Cerckel, G., Damoczi, J., Ledesma-Garcia, L., Sass, A., Coenye, T., Nessler, S., and Hols, P. (2019). Subtle selectivity in a pheromone sensor triumvirate desynchronizes competence and predation in a human gut commensal. Elife *8*, e47139. https://doi.org/10.7554/eLife.47139.
29. Mignolet, J., Fontaine, L., Sass, A., Nannan, C., Mahillon, J., Coenye, T., and Hols, P. (2018). Circuitry Rewiring Directly Couples Competence to Predation in the Gut Dweller Streptococcus salivarius. Cell Rep. *22*, 1627–1638. https://doi.org/10.1016/j.celrep.2018.01.055.
30. Ma, S., Zhao, Y., Xia, X., Dong, X., Ge, W., and Li, H. (2015). Effects of Streptococcus sanguinis Bacteriocin on Cell Surface Hydrophobicity, Membrane Permeability, and Ultrastructure of Candida Thallus. BioMed Res. Int. *2015*, 514152. https://doi.org/10.1155/2015/514152.
31. Fujimura, S., and Nakamura, T. (1979). Sanguicin, a bacteriocin of oral Streptococcus sanguis. Antimicrob. Agents Chemother. *16*, 262–265. https://doi.org/10.1128/AAC.16.3.262.
32. Rodriguez, A.M., Callahan, J.E., Fawcett, P., Ge, X., Xu, P., and Kitten, T. (2011). Physiological and molecular characterization of genetic competence in Streptococcus sanguinis. Mol. Oral Microbiol. *26*, 99–116. https://doi.org/10.1111/j.2041-1014.2011.00606.x.
33. Harrington, A., and Tal-Gan, Y. (2018). Identification of Streptococcus gallolyticus subsp. gallolyticus (Biotype I) Competence-Stimulating Peptide Pheromone. J. Bacteriol. *200*, e00709–e00717. https://doi.org/10.1128/JB.00709-17.
34. Mull, R.W., and Tal-Gan, Y. (2021). Elucidating the Role and Structure-Activity Relationships of the Streptococcus oligofermentans Competence-Stimulating Peptide. ACS Chem. Biol. *16*, 2834–2844. https://doi.org/10.1021/acschembio.1c00746.
35. Prudhomme, M., Berge, M., Martin, B., and Polard, P. (2016). Pneumococcal Competence Coordination Relies on a Cell-Contact Sensing Mechanism. PLoS Genet. *12*, e1006113. https://doi.org/10.1371/journal.pgen.1006113.
36. Son, M., Ahn, S.J., Guo, Q., Burne, R.A., and Hagen, S.J. (2012). Microfluidic study of competence regulation in Streptococcus mutans: environmental inputs modulate bimodal and unimodal expression of comX. Mol. Microbiol. *86*, 258–272. https://doi.org/10.1111/j.1365-2958.2012.08187.x.
37. Cassone, M., Gagne, A.L., Spruce, L.A., Seeholzer, S.H., and Sebert, M.E. (2012). The HtrA protease from Streptococcus pneumoniae digests both denatured proteins and the competence-stimulating peptide. J. Biol. Chem. *287*, 38449–38459. https://doi.org/10.1074/jbc.M112.391482.
38. Hossain, M.S., and Biswas, I. (2012). An extracelluar protease, SepM, generates functional competence-stimulating peptide in Streptococcus mutans UA159. J. Bacteriol. *194*, 5886–5896. https://doi.org/10.1128/JB.01381-12.
39. Harrington, A., Proutière, A., Mull, R.W., du Merle, L., Dramsi, S., and Tal-Gan, Y. (2021). Secretion, Maturation, and Activity of a Quorum Sensing Peptide (GSP) Inducing Bacteriocin Transcription in Streptococcus gallolyticus. mBio *12*, 031899–e3220. https://doi.org/10.1128/mBio.03189-20.
40. Petersen, F.C., Fimland, G., and Scheie, A.A. (2006). Purification and functional studies of a potent modified quorum-sensing peptide and a two-peptide bacteriocin in Streptococcus mutans. Mol. Microbiol. *61*, 1322–1334. https://doi.org/10.1111/j.1365-2958.2006.05312.x.
41. Wang, C.Y., Patel, N., Wholey, W.Y., and Dawid, S. (2018). ABC transporter content diversity in Streptococcus pneumoniae impacts competence regulation and bacteriocin production. Proc. Natl. Acad. Sci. USA *115*, E5776–E5785. https://doi.org/10.1073/pnas.1804668115.
42. Terleckyj, B., and Shockman, G.D. (1975). Amino acid requirements of Streptococcus mutans and other oral streptococci. Infect. Immun. *11*, 656–664. https://doi.org/10.1128/iai.11.4.656-664.1975.
43. Milly, T.A., Buttner, A.R., Rieth, N., Hutnick, E., Engler, E.R., Campanella, A.R., Lella, M., Bertucci, M.A., and Tal-Gan, Y. (2022). Optimizing CSP1 analogs for modulating quorum sensing in Streptococcus pneumoniae with bulky, hydrophobic nonproteogenic amino acid substitutions. RSC Chem. Biol. *3*, 301–311. https://doi.org/10.1039/d1cb00224d.
44. Milly, T.A., Engler, E.R., Chichura, K.S., Buttner, A.R., Koirala, B., Tal-Gan, Y., and Bertucci, M.A. (2021). Harnessing Multiple, Nonproteogenic Substitutions to Optimize CSP:ComD Hydrophobic Interactions in Group 1 Streptococcus pneumoniae. Chembiochem *22*, 1940–1947. https://doi.org/10.1002/cbic.202000876.
45. Milly, T.A., and Tal-Gan, Y. (2020). Biological Evaluation of Native Streptococcal Competence Stimulating Peptides Reveal Potential Crosstalk Between Streptococcus mitis and Streptococcus pneumoniae and a New Scaffold for the Development of S. pneumoniae Quorum Sensing Modulators. RSC Chem. Biol. *1*, 60–67. https://doi.org/10.1039/D0CB00012D.
46. Loh, J.M.S., and Proft, T. (2013). Toxin-antitoxin-stabilized reporter plasmids for biophotonic imaging of Group A streptococcus. Appl. Microbiol. Biotechnol. *97*, 9737–9745. https://doi.org/10.1007/s00253-013-5200-7.
47. Guo, M., Ye, L., Yu, T., Han, L., Li, Q., Lou, P., Gan, T., Jin, X., Xiao, H., Meng, G., et al. (2020). IL-1beta Enhances the Antiviral Effect of IFN-alpha on HCV Replication by Negatively Modulating ERK2 Activation. ACS Infect. Dis. *6*, 1708–1718. https://doi.org/10.1021/acsinfecdis.9b00506.
48. Garcia-Gutierrez, E., O'Connor, P.M., Saalbach, G., Walsh, C.J., Hegarty, J.W., Guinane, C.M., Mayer, M.J., Narbad, A., and Cotter, P.D. (2020). First evidence of production of the lantibiotic nisin P. Sci. Rep. *10*, 3738. https://doi.org/10.1038/s41598-020-60623-0.

Please cite this article in press as: Guo et al., Noncanonical *Streptococcus sanguinis* ComCDE circuitry integrates environmental cues in transformation outcome decision, Cell Chemical Biology (2023), https://doi.org/10.1016/j.chembiol.2023.09.007





## STAR★METHODS

### KEY RESOURCES TABLE

| REAGENT or RESOURCE | SOURCE | IDENTIFIER |
|---|---|---|
| Bacterial and virus strains | | |
| *S. sanguinis* wildtype VMC66 | BEI Resources | VMC66 |
| VMC66::Φ($P_{tur}$-*comC*), SpecR | This study | WT ComC |
| VMC66::Φ($P_{tur}$-*comC*), Δ*comCDE*, SpecR, EryR | This study | WT ComC + Δ*comCDE* |
| VMC66::Φ($P_{tur}$-*comC*), Δ*comX*, SpecR, EryR | This study | WT ComC+ Δ*comX* |
| VMC66::Φ($P_{tur}$-*comC* del 2-5), SpecR | This study | ComC del 2-5 |
| VMC66::Φ($P_{tur}$-*comC* del 2-9), SpecR | This study | ComC del 2-9 |
| VMC66::Φ($P_{tur}$-*comC* del 2-14), SpecR | This study | ComC del 2-14 |
| VMC66::Φ($P_{tur}$-*comC* del 2-17), SpecR | This study | ComC del 2-17 |
| VMC66::Φ($P_{tur}$-*comC* del 2-20), SpecR | This study | ComC del 2-20 |
| VMC66::Φ($P_{tur}$-*comC* del 15-20), SpecR | This study | ComC del 15-20 |
| VMC66::Φ($P_{tur}$-*comC* W20A), SpecR | This study | ComC W20A |
| VMC66::Φ($P_{tur}$-*comC* F19A), SpecR | This study | ComC F19A |
| VMC66::Φ($P_{tur}$-*comC* T18A), SpecR | This study | ComC T18A |
| VMC66::Φ($P_{tur}$-*comC* Q17A), SpecR | This study | ComC Q17A |
| VMC66::Φ($P_{tur}$-*comC* V16A), SpecR | This study | ComC V16A |
| VMC66::Φ($P_{tur}$-*comC* L15A), SpecR | This study | ComC L15A |
| VMC66::Φ($P_{tur}$-*comC* del35), SpecR | This study | ComC del35 |
| VMC66 A1 cluster deletion, SpecR | This study | ΔA1 |
| VMC66 Δ94975, SpecR | This study | ΔA2-1 |
| VMC66 Δ94976, SpecR | This study | ΔA2-2 |
| VMC66 Δ94977, SpecR | This study | ΔA2-3 |
| VMC66 ΔA3 cluster, SpecR | This study | ΔA3 |
| VMC66 Δ94247, SpecR | This study | ΔA3-1 |
| VMC66 Δ94250, SpecR | This study | ΔA3-2 |
| VMC66 ΔA4 cluster, SpecR | This study | ΔA4 |
| VMC66 ΔA5 cluster, SpecR | This study | ΔA5 |
| VMC66 ΔA6 cluster, SpecR | This study | ΔA6 |
| VMC66 ΔA7 cluster, SpecR | This study | ΔA7 |
| VMC66::Φ($P_{comYA}$OroP), EryR | This study | RT |
| VMC66 ΔA1 cluster::Φ($P_{comYA}$OroP), EryR, SpecR | This study | ΔA1+RT |
| VMC66 Δ94975::Φ($P_{comYA}$OroP), EryR, SpecR | This study | ΔA2-1 +RT |
| VMC66 Δ94976::Φ($P_{comYA}$OroP), EryR, SpecR | This study | ΔA2-2 +RT |
| VMC66 Δ94977::Φ($P_{comYA}$OroP), EryR, SpecR | This study | ΔA2-3 +RT |
| VMC66 ΔA3 cluster::Φ($P_{comYA}$OroP), EryR, SpecR | This study | ΔA3+RT |
| VMC66 Δ94247::Φ($P_{comYA}$OroP), EryR, SpecR | This study | ΔA3-1+RT |
| VMC66 Δ94250::Φ($P_{comYA}$OroP), EryR, SpecR | This study | ΔA3-2+RT |

(*Continued on next page*)

Please cite this article in press as: Guo et al., Noncanonical *Streptococcus sanguinis* ComCDE circuitry integrates environmental cues in transformation outcome decision, Cell Chemical Biology (2023), https://doi.org/10.1016/j.chembiol.2023.09.007



***Continued***

| REAGENT or RESOURCE | SOURCE | IDENTIFIER |
|---|---|---|
| VMC66 ΔA4 cluster::Φ($P_{comYA}$OroP), EryR, SpecR | This study | ΔA4+RT |
| VMC66 ΔA5 cluster::Φ($P_{comYA}$OroP), EryR, SpecR | This study | ΔA5+RT |
| VMC66 ΔA6 cluster::Φ($P_{comYA}$OroP), EryR, SpecR | This study | ΔA6+RT |
| VMC66 ΔA7 cluster::Φ($P_{comYA}$OroP), EryR, SpecR | This study | ΔA7+RT |
| VMC66 Δ94247, 95200::(94247,94248,94249), EryR, SpecR | This study | ΔA3-1-res |
| VMC66 Δ94977, 95200::94977, EryR, SpecR | This study | ΔA2-3-res |
| VMC66 Δ94247, 95200::(94247,94248,94249), Φ($P_{comYA}$OroP), EryR, SpecR, CatR | This study | ΔA3-1-res+RT |
| VMC66 Δ94977 95200::94977,Φ($P_{comYA}$OroP), EryR, SpecR, CatR | This study | ΔA2-3-res+RT |
| VMC66 Δ*comCDE*, SpecR | This study | Δ*comCDE* |
| VMC66 Δ*comX*, SpecR | This study | Δ*comX* |
| VMC66 Δ94247, Δ94977, EryR, SpecR | This study | ΔA2-3 +ΔA3-1 |
| VMC66 Δ*spxB*, SpecR | This study | Δ*spxB* |
| VMC66::Φ($P_{comCDE}$*luc*), SpecR | This study | $P_{comcde}$luc |
| VMC66 Δbacteriocin biosynthesis cluster, SpecR | This study | Δbacteriocin cluster |
| VMC66::95200(*comDE*), Δ*comCDE*, EryR, CatR | This study | Δ*comC* |
| VMC66::95200(*comDE*), Δ*comCDE*, Φ($P_{comCDE}$*luc*), SpecR, EryR, CatR | This study | Δ*comC* Luc |
| VMC66::95200($P_{comCDE}$*luc*), Φ($P_{tuf}$-*comC* del 2-20), SpecR, EryR | This study | ComC del 2-20+$P_{comCDE}$*luc* |
| VMC66::95200($P_{comCDE}$*luc*), Φ($P_{tuf}$-*comC*), SpecR, EryR | This study | WT ComC+ $P_{comCDE}$*luc* |
| **Recombinant DNA** | | |
| pDL278-$P_{tuf}$ComC | This study | N/A |
| pFW11-$P_{comCDE}$luc | This study | N/A |
| pFW11-$P_{comYA}$OroP-Spec | This study | N/A |
| pFW11-$P_{comYA}$OroP-Ery | This study | N/A |
| pFW11-$P_{comYA}$OroP-Cat | This study | N/A |
| **Oligonucleotides** | | |
| See Data S2. | This study | N/A |
| **Chemicals, peptides, and recombinant proteins** | | |
| H-DLRGVPNPWGWIFGR-OH | This study | N/A |
| H-RGVPNPWGWIFGR-OH | This study | N/A |
| H-LRGVPNPWGWIFGR-OH | This study | N/A |
| H-WDLRGVPNPWGWIFGR-OH | This study | N/A |
| H-FWDLRGVPNPWGWIFGR-OH | This study | N/A |
| H-TFWDLRGVPNPWGWIFGR-OH | This study | N/A |
| H-QTFWDLRGVPNPWGWIFGR-OH | This study | N/A |
| H-VQTFWDLRGVPNPWGWIFGR-OH | This study | N/A |
| H-VQTFWDLRGVPNPWGWIFGR-OH | This study | N/A |
| H-DL($d_{10}$)RGVPNPWGWIFGR-OH | This study | N/A |

(*Continued on next page*)

*Continued*

| REAGENT or RESOURCE | SOURCE | IDENTIFIER |
|---|---|---|
| H-DLRGVPNPWGWIFG-OH | This study | N/A |
| Deposited data | | |
| Sequence of pDL278-$P_{tuf}$ComC | This study | GenBank: OR518276 |
| Sequence of pFW11-$P_{comCDE}$luc | This study | GenBank: OR518278 |
| Sequence of pFW11-$P_{comYA}$OroP-Spec | This study | GenBank: OR518279 |
| Sequence of pFW11-$P_{comYA}$OroP-Ery | This study | GenBank: OR518277 |
| Sequence of pFW11-$P_{comYA}$OroP-Cat | This study | GenBank: OR518280 |
| Software and algorithms | | |
| GraphPad Prism 9 | GraphPad | https://www.graphpad.com/ |

## RESOURCE AVAILABILITY

### Lead contact

Further information and requests for resources and reagents should be directed to and will be fulfilled by the lead contact, Dr. Yftah Tal-Gan (ytalgan@unr.edu).

### Materials availability

Strains and reagents used in this study are available upon request from Dr. Yftah Tal-Gan.

### Data and code availability

- The sequences of plasmid constructs created in this study are deposited in GenBank and accession numbers are listed in the key resources table. Data reported in this study will be shared by the lead contact upon request.
- The paper does not report original code.
- Any additional information required to analyze the data reported in this paper is available from the lead contact upon request.

## EXPERIMENTAL MODEL AND STUDY PARTICIPANT DETAILS

### Bacterial growth

All *S. sanguinis* cultures were grown in THY media at 37°C with 5% $CO_2$. *E. coli* cultures were grown in SOB media at 37°C with shaking. For selection in THY, the following antibiotics were used: spectinomycin (300 mg/L), erythromycin (5 mg/L), chloramphenicol (4 mg/L). For selection in LB media, the following antibiotics were used: spectinomycin (50 mg/L), erythromycin (250 mg/L). The C+Y media used in this study was based on a Chemically Defined Media (CDM) recipe previously described,[42] supplemented with 2.2 g yeast extract per liter.

### Strain construction

All strains generated in this study are listed in the key resources table. Chromosomal insertions and deletions in *S. sanguinis* were achieved through homologous recombination with linear DNA cassette consisting of the two flanking 1000-bp fragments upstream and downstream of the designated insertion site and the suitable antibiotic selection marker or other payload sequence sandwiched between the flanking fragments. In details, the linear knockout cassette was assembled and amplified with overlapping PCR. As for complementation of the ΔA3-1 transporter strain, the original locus containing the native promoter and ORFs of 94247, 94248, and 94249 were inserted in a permissive locus (VMC66, 95200). The primers RE F5, RE F3, RE R5 and RE R3 were used to amplify the flanking regions from genomic DNA. The erythromycin resistance cassette was amplified from the blank pUC19 vector with primers RE ery5 and RE ery3. The native A3-1 cluster was amplified with primers A3r5 and A3r3, and the target integration cassette was obtained through overlapping PCR with primer set RE F5 and RE R3. The same strategy was used for the ΔA2-3 rescue. The transformation of plasmid and linear DNA cassettes were achieved with CSP-induced competence protocol from a previous study.[32] Briefly, an overnight culture of S. sanguinis was diluted 1:200 with fresh THY. An aliquot of 500 μL of diluted culture was transferred to a sterile glass tube and mixed with CSP (113 nM) and target DNA. After incubation at 37°C with 5% CO2 for another 90 min, the culture was streaked on THY plates supplemented with the appropriate antibiotic concentration. Colony formation was assessed after two days.

Please cite this article in press as: Guo et al., Noncanonical *Streptococcus sanguinis* ComCDE circuitry integrates environmental cues in transformation outcome decision, Cell Chemical Biology (2023), https://doi.org/10.1016/j.chembiol.2023.09.007



## METHOD DETAILS

### Solid-phase peptide synthesis, HPLC, and mass spectrometry

Peptide synthesis and purification was executed with previously established methods.[43–45] All peptides used in this study were purified to homogeneity (over 95% purity, Data S1) and were characterized with Agilent Technologies 6230 time-of-flight high-resolution mass spectrometer (HRMS). The characterization of the peptides used in this study is shown in Data S1 and Table S1. Reverse phase high-performance liquid chromatography (RP-HPLC) was performed using a Shimadzu UFLC system. All RP-HPLC solvents ($H_2O$ and acetonitrile) were supplemented with 0.1% trifluoroacetic acid (TFA). Preparative RP-HPLC was performed using a Phenomenex Kinetex 5-μm, 100-Å C18 column (250 by 10 mm), with a linear gradient of 25% to 40% ACN over 25 min and a flow rate of 5 mL/min. Analytical HPLC was performed using a Phenomenex Kinetex 5-μm, 100-Å C18 column (250 by 4.6 mm), with a linear gradient of 5% to 95% ACN over 25 min and a flow rate of 1 mL/min. MALDI-TOF-MS (Matrix-assisted laser desorption ionization time-of-flight mass spectrometry) data were obtained by mixing 0.75 μL of sample with 0.75 μL of matrix solution (α-cyano-4-hydroxycinnamic acid dissolved in $H_2O$:ACN [1:1] with 0.1% TFA) on an MSP 96 polished steel target plate (Bruker Daltonics). Data were obtained using a Bruker Microflex spectrometer equipped with a 60 Hz (337 nm wavelength) nitrogen laser and a reflectron. Exact mass (EM) data were obtained on an Agilent Technologies 6230 time-of-flight mass spectrometer (TOF-MS) connected with a XBridge C18 column. Mobile phase A is dd$H_2O$ with 0.1% formic acid, mobile phase B is ACN with 0.1% formic acid, a linear gradient of mobile phase B from 5% to 95% over 25 minutes was used (0.5 ml/min). The injection volume of the samples was 100 μL where peptide concentrations were adjusted to about 0.1 μM.

### Isolation of native *S. sanguinis* CSP

*S. sanguinis* single colony was inoculated in 50 mL of THY at 37°C with 5% $CO_2$ for 16 h. Then, 25 mL overnight culture was added into 175 mL fresh THY and incubated at 37°C with 5% $CO_2$ for 30 min. Next, 5 mg synthetic peptides were added into the newly prepared diluted culture. After thorough mixing, the treated culture was incubated at 37°C with 5% $CO_2$ for 20 min. Then, the culture was centrifuged at 4,000 rpm for 30 min, the supernatant was filtered by a 0.22 μm filter. Next, ammonium sulfate (40% [wt/vol]) was added to the clear supernatant to precipitate the total peptide content. The mixture was centrifuged at 4,000 rpm at 4°C for 30 min after incubating at 4°C overnight. The crude protein pellet was resuspended in 30 mL 1:9 ACN:water. After filtering with 0.45 μm syringe filter, 1 mL of the clear crude peptide was injected onto a preparative HPLC column with a linear gradient of 25% to 40% ACN over 25 min and a flow rate of 5 mL/min. The peptide contents in each fraction were characterized with MALDI-TOF-MS and further verified via EM measurement. Native *S. sanguinis* CSP (purity >99%) was obtained after four consecutive rounds of preparative HPLC purification. MS/MS analysis of the extracted and synthetic peptides was performed on a ThermoFisher Orbitrap Fusion Tribrid Mass Spectrometer. Peptide solutions were prepared to final concentrations of ~0.5-1.0 μM using 1% Formic Acid in 50:50 Methanol:$H_2O$ (mass spectrometry grade), by passing them through a 0.45 μm filter to remove fine particulates. The two peaks with the strongest intensity ($MH^{+2}$ and $MH^{+3}$) from the MS data were chosen for MS/MS fragmentation and isolated via quadrupole isolation. During MS/MS analysis, the Orbitrap detector was used with the resolution set to 120,000. The higher energy collisionally activated dissociation (HCD) energy was scanned from 0-45% (data not shown) at intervals of 5% to determine the HCD energy range for optimal peptide fragmentation. The HCD energy for the final MS/MS fragmentation was set to 38% and 18% for the $MH^{+2}$ and $MH^{+3}$ ions, respectively, for both the extracted and synthetic peptides. The spectral data for MS and MS/MS were copied to Microsoft Excel and analyzed in Origin Pro.

### Luminescence assays

For luciferase assays, the *S. sanguinis* VMC66 $P_{comCDE}$luc overnight culture was used to prepare fresh diluted culture at 1:10 ratio, which was then incubated at 37°C with 5% $CO_2$ for 30 min. Then, 198 μL diluted culture was aliquoted into the wells of white 96-well microtiter plate. Two μL of DMSO or serially diluted synthetic peptides were added to each of the wells. After mixing, the plate was then incubated at 37°C with 5% $CO_2$ for another 20 min. Next, luminescence signal was measured with a Biotek Synergy H1 microplate reader using Gen5 data analysis software (v. 3.03). $EC_{50}$ values from three independent experiments were calculated using GraphPad Prism7.

### Plasmid construction

PCR amplification was performed with Q5 DNA polymerase (NEB, Ipswich, MA, USA) at cycling parameters recommended in user manuals. The primers used in this study are listed in Data S2. To construct $P_{comCDE}$luc reporter, the S. sanguinis *comCDE* promoter was amplified with primers pComCDE-F and pComCDE-R. The blank pFW11 vector[46] with spectinomycin marker was linearized with primers lucbac-F and lucbac-R. The primer design ensures the comCDE promoter was inserted directly before the luciferase gene start codon. The two fragments were mixed in an equimolar ratio and assembled with HiFi DNA assembly reagent from NEB. The final construct was named pComCDE-luc-pFW11-spec. To construct competence-coupled toxicity reporter, the OroP ORF[29] was amplified with primers OroP-F and OroP-R, the promoter of late competence gene comYA was amplified with primers pComYA-F and pComYA-R. The blank pFW11 vector was linearized with primers B1F and B1R. The primer design ensures the OroP was inserted immediately following the comYA promoter. The PcomYAOroP-pFW11-spec was obtained after first round ligation. To change to antibiotic marker of the construct, the backbone was linearized with primer B2F and B2R. Concurrently, an erythromycin resistance marker was amplified from blank pUC19 vector with primers Ery5 and Ery3. After the second round of ligation, the product pComYA-

OroP-pFW11-ery was derived. For constitutive ComC expression plasmid series, the full ComC ORF was amplified with primer ComC5 and ComC3 with genomic DNA extracted from *S. sanguinis* VMC66. The constitutive promoter of the housekeeping gene *tuf* was amplified with primers pTuf5 and pTuf3. The pDL278 backbone was linearized with primers B3F and B3R. The three fragments were then assembled so that ComC was immediately after the tuf promoter, producing the final construct pTuf-ComC-pDL278-spec. ComC expression constructs with mutations and truncations were generated using the same strategy. All constructs were verified with Sanger sequencing. Complete sequences of plasmid series created in this study are deposited in GenBank, accession numbers are listed in the key resources table.

### RNA isolation and quantification

The RNA extraction was carried out as previously described with several modifications.[47] Briefly, bacterial pellet was dissolved in RNA lysis buffer (50 mM sodium acetate buffer, 10 mM EDTA and 5% SDS, w/v, pH 5.5), which was mixed with 300 mg of 0.1 mm glass beads and equal volume of 1:1 phenol-chloroform mixture in a 2 mL screw cap tube. The bacteria were then lysed with FastPrep-24 homogenizer (MP Biomedicals) per recommended program from manufacturer. After centrifugation, the clear aqueous phase was mixed with equal volume of isopropanol. After centrifugation at 4°C, 20,000 g for 10 min, the pellet was washed twice with DEPC-treated 70% ethanol. Then, the dissolved RNA was treated with DNaseI (Invitrogen, Thermo Fisher Scientific) for 1 h. The pure RNA was obtained after secondary phenol-chloroform extraction. The cDNA synthesis was performed with LunaScript RT SuperMix Kit (NEB). Quantitative real-time PCR was performed with Luna Universal qPCR Master Mix (NEB) on a Bio-rad CFX96 Touch Real-Time PCR Detection System. The mRNA levels of various target genes were normalized to the mRNA level of the *S. sanguinis* housekeeping gene *tuf*.

### Competition assays on solid medium

To assess the antimicrobial activity of the bacteriocin in spent *S. sanguinis* media, we used a spot-on-lawn assay. Briefly, 20 μL overnight culture of various microbes were mixed with 180 μL fresh THY media and evenly streaked on a THY plate without any antibiotics as an indicator layer. When the indicator layer was completely absorbed by the agar, 5 μL of the putative bacteriocin culture was spotted on the top of the indicator layer (10 mg crude peptide extract containing bacteriocin was dissolved with 198 μL fresh THY media and 2 μL DMSO). Then, the THY plate was incubated at 37°C for 16 hours with 5% $CO_2$, followed by the assessment of the presence of an inhibition halo.

### Quantification of CSP concentration in spent bacterial culture

The overnight culture of various *S. sanguinis* strains were diluted with a ratio of 1 to 10. After 1h incubation, 100ng synthetic CSP was added to the diluted *S. sanguinis* culture, the supernatant was collected 20min after CSP treatment. After removing the cell debris with a 0.22 μm filter, the supernatant was stored at 4°C. To quantify the CSP concentration in spent media. First, a luminescence-CSP response standard curve was created with *S. sanguinis* $P_{comCDE}$luc, ΔcomC reporter strain. Next, spent media from various *S. sanguinis* backgrounds was diluted serially, and quantified with the reporter strain. Finally, the CSP concentration was determined with the supernatant having the appropriate dilution ratio where luminescence is within the linear range of the standard curve.

### Measurement of growth defect

5-Fluoroorotic acid (5-FOA) induced artificial toxicity assays were setup as follows. The S. sanguinis ABC transporter knockout strains were transformed with the toxicity reporter, then fresh colonies of respective strains harboring toxicity reporter were inoculated into THY media supplemented with erythromycin (5 mg/L). The next day, overnight cultures were diluted 1:200 with fresh THY supplemented with erythromycin (5 mg/L) and three 198 μL aliquots were transferred to wells in a 96-well-plate. Then 2 μL DMSO or 5-FOA (final concentration 1 mg/mL) was added to the diluted cultures. The plate was then transferred to the incubator at 37°C with 5% CO2, and the endpoint OD600 values were recorded after 12 h. For the ComC induced growth inhibition assay, the experiment setup was as follows. For synthetic CSP treatment group, the WT S. sanguinis overnight culture was diluted 1:500 with fresh THY media and three 198 μL aliquots were transferred to wells in a 96-well-plate, then 2 μL DMSO or CSP was added to the diluted cultures. For *S. sanguinis* strain harboring constitutive ComC expression, the overnight culture was diluted 1:500 with fresh THY media and three 198 μL aliquots were transferred to wells in a 96-well-plate. Growth curves were plotted with hourly OD600 values over 27 hours from three independent replicates.

### Isolation of *S. sanguinis* bacteriocin

*S. sanguinis* bacteriocin purification was adapted from a previous study.[48] A single *S. sanguinis* colony was inoculated in 400 mL fresh THY and incubated at 37°C with 5% CO2. After overnight incubation, the spent culture was centrifuged at 4,000 rpm for 30 min, and the supernatant was filtered by a 0.22 μm filter. Next, ammonium sulfate (40% [wt/vol]) was added to the clear supernatant to precipitate the total peptide content. The mixture was centrifuged at 4,000 rpm at 4°C for 30 min after incubating at 4°C overnight. The crude protein pellet was resuspended in 30 mL 1:9 ACN:water. After filtering with 0.45 μm syringe filter, 1 mL of the clear crude peptide was injected onto a preparative HPLC column with a linear gradient of 20% to 40% ACN over 25 min and a flow rate of 5 mL/min. The fractions eluted at 23-26% ACN were combined and lyophilized. After first round of lyophilization,

the peptide was dissolved with 2 mL ACN:AcOH:Water 37.5:37.5:25. After a second round of lyophilization, the crude peptide was weighed and 10 mg of the end product was dissolved with 198 μL fresh THY media and 2 μL DMSO.

### Assessment of antimicrobial capability of spent media

A single S. sanguinis colony of respective genetic background was inoculated in 100 mL fresh THY and incubated at 37°C with 5% CO2 overnight. The spent culture was centrifuged at 4,000 rpm for 30 min, and the supernatant was filtered by a 0.22 μm filter. Next, ammonium sulfate (50% [wt/vol]) was added to the clear supernatant to precipitate the total peptide content. The mixture was centrifuged at 4,000 rpm at 4°C for 30 min after incubating at 4°C overnight. The crude protein pellet was dissolved with 4 mL 1:9 ACN:-water, and 1 mL 0.45 μm-filtered crude peptide was injected onto a preparative HPLC column. The elution gradient was 10% to 40% ACN over 25 min and a flow rate of 5 mL/min, and in this ACN range, each fraction was collected with a fixed duration of 80 seconds. The initial fractions were frozen and lyophilized, and the content within the glass vials was dissolved with 2 mL ACN:AcOH:Water 37.5:37.5:25. After a second round of lyophilization, the crude peptide was dissolved with 198 μL fresh THY media and 2 μL DMSO. Fifty μL of the resuspended crude peptide from each fraction was mixed with 150 μL 1:1000 diluted L. lactis overnight culture. The mixture was then transferred into wells of clear 96-well plate in triplicate. The plate was loaded into a BioSpa automated incubator at 37°C with 5% CO2 (BioTek, Agilent), where OD600 was recorded every 60 minutes for 18 hours.

## QUANTIFICATION AND STATISTICAL ANALYSIS

All statistical analyses were performed with GraphPad Prism 9. Means between groups were compared using two-tailed unpaired Student's t-test. For comparison of multiple groups with one variable, one-way ANOVA variance analysis was performed. Data are displayed as mean ± SD. Statistically significance of data are indicated: ns, not significant, * $P < 0.05$.